ISSN Application No. 21825

Journal of Applied Physics

Volume No. 11

Issue No. 3

September - December 2023

ENRICHED PUBLICATIONS PVT. LTD

S-9, IInd FLOOR, MLU POCKET,
MANISH ABHINAV PLAZA-II, ABOVE FEDERAL BANK,
PLOT NO-5, SECTOR-5, DWARKA, NEW DELHI, INDIA-110075,
PHONE: - + (91)-(11)-47026006

ISSN Application No. 21825

Journal of Applied Physics

Aims and Scope

The Journal of Applied Physics is published tri-annually Enriched publications. Journal of Applied Physics is peer reviewed journal and monitored by a team of reputed editorial board members. This journal consists of research articles, reviews, and case studies on Science Technology. This journal mainly focuses on the latest and most common subjects of its domain.

ISSN Application No. 21825

Journal of Applied Physics

ISSN Application No. 21825

Journal of Applied Physics

(Volume No. 11, Issue No.3, September-December 2023)

Contents

Sr. No	Articles/ Authors	Pg No
01	Creep and Hardness Property Study for UHMWPE Composites using Nano Indentation - *Ravivardhan N A* , Prof. T. Jagadish**	115 - 124
02	Modulus of Elasticity for Steel Fibre Reinforced Recycle Aggregate Concrete - *C. Sashidhar, .Venkata Subbareddy, N. Venkata Ramana*	125 - 134
03	Reliability Assessment of Flat Slab Building using Pushover Analysis - *Nikhil P, Rekha B*	135 - 142
04	Diagnosing the Faulty Model of A Motor Based on Fft Analyzer with Vibrating Analysis - *Bharathi S L, N. Pritha, N. Arunpriya, R. Preethi , A. Murali*	143 - 150
05	Modeling and Control of Fuel Cell Power Plant Using PID Controller - *Satish Kumar, Govind Kumar Maurya*	151 - 159

Creep and Hardness Property Study for UHMWPE Composites using Nano Indentation

Ravivardhan N A*, Prof. T. Jagadish**

* Doctorate Program, Department of Mechanical Engineering, Bangalore Institute of Technology, Bangalore, India Email: ravi.scbose@gmail.com

** Professor and Head, Department of Mechanical Engineering, Bangalore Institute of Technology, Bangalore, India

ABSTRACT

Ultra high molecular weight polyethylene (UHMWPE) is used as articulating surface material for hip joint replacements. Due to permanent deformation of material it leads to dislocation of artificial hip joint. Composite material was developed by blending UHMWPE with varying percentage of Multi walled carbon nanotubes reinforcement. This blended mixture of material is compressed in compression molding machine to get sheets. Hardness and Creep tests were carried on Composite specimens and the results were compared and validated using Oliver and Pharr analytical model. It is observed that, as the weight percentage of multiwall carbon nanotube is increased the hardness increases up to 25% and creep displacement decreases up to 29% when compared with pure Ultra high molecular weight polyethylene material.

Keywords: Creep; Hardness; NanoIndentation; UHMWPE; MWCNT.

1. INTRODUCTION

In the past, different materials are studied and reviewed for bearing surfaces applications. Biologically there are few reasons because of which hip joint fails and lead to hip joint replacement as explained by S. Ramakrishna et al [1]. George Matsoukas et al [2] stated liberation of wear particles at articulate surfaces of hip joint lead to inflammatory defined as Osteolysis. Also permanent deformation due to creep effect leads to dislocation of hip joint. The solution is to develop composite materials with improved Creep, Stiffness and Hardness properties. Ultra high molecular weight polyethylene material has excellent properties like high wear resistance, strength, chemical stability and bio compatibility. Thus it is used for Total hip replacement from many years [3-5].

Creep displacement of Ultra high molecular weight polyethylene is higher than conventional metals which introduce the gap between acetabula cup and femoral head leading to loosening of the hip joint and dislocation failure. Also, Wear debris liberation of Ultra high molecular weight polyethylene material lead to loosening of implants which in turn cause the long term failure of Total hip joint replacement [7]. Hence study is carried out to improve the creep, hardness and modulus properties of Ultra high molecular weight polyethylene by blending multi wall carbon Nano tube to increased life span of Total hip joint replacement. The objective of the present study is to compare the creep displacement, hardness and reduced modulus property of pure Ultra high molecular weight polyethylene with multiwall carbon nanotube blended with Ultra high molecular weight polyethylene composite material. The essence of the present work is to get an idea regard the effect of Multi walled carbon nano tube (MWCNT) reinforcement variation on Creep and Hardness properties. Experimental results are validated by Oliver and Pharr analytical model.

2. PREPARATION OF COMPOSITE

Multi walled carbon nano tubes (MWCNT's) are used as filler material along with Ultra high molecular weight polyethylene for the preparation of composites sheet. Multi walled carbon nano tubes has the dimensions of outer diameter ranging from 8 to 15 nm, length 10 to 50 µm having density of 2100 Kg/m3 (2.1 g/cm3) and the purity was reported to be more than 95% with an ash content of 1.5%. Ultra-high molecular weight polyethylene with molecular weight ranging from 3.5 x 106 to 6 x 106 g/mol (ASTM calculation) is used as base material. Ultra-high molecular weight polyethylene will be in the form of powder with particle size ranging from 0 - 500µm, with an average size in the range of 135- 150 µm. The density of Ultra-high molecular weight polyethylene powder is 930 Kg/m^3. Chemically treated Multi walled carbon nano tubes (MWCNTs) and Ultra-high molecular weight polyethylene (UHMWPE) was physically blended using Plastic corder machine shown in Figure-1 for 30 minutes. The temperature of the compound inside the chamber is maintained at 200^0 C. The "dough" obtained after melt-mixing the powder were put in the die.

During compaction stage, temperature of the die plates was also maintained at 200^0 C and the material is first compressed to 19 MPa (190 bar) for one minute. The die is unloaded to allow recrystallization of the material o at 200^0C. Further the die is loaded again to attain a pressure of 19 MPa (190 bar) for five minutes. Machine used for this purpose is shown in Figure-2. Finally die is unloaded and water cooled to room temperature before the composite sheets are removed. The size of compression molded sheets is 150 x 150 x 2mm which is shown in Figure 3.

Figure 1.Brabender Machine

Figure 2. Hot Press Machine

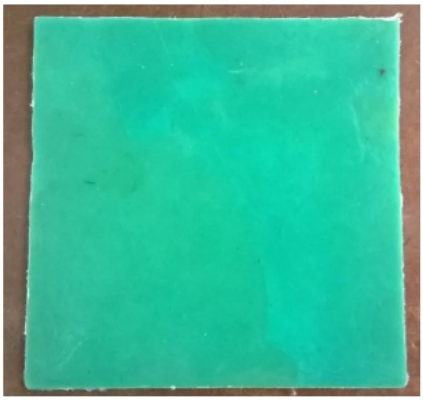

Figure 3. Compression moulded Ultra-High Molecular Weight Polyethylene sheet

3. HARDNESS TEST

Hardness test is performed using Keysight Nano indenter G200 make. Tests were performed for UHMWPE, UHMWPE + 1% CNT, UHMWPE + 3% CNT and UHMWPE + 5% CNT materials. The Specimen is sized to dimension of 25mm x 25mm and test surface are cleaned. Nano indentation was performed using Berkovich diamond indenter. Test is carried out by applying load in milli Newton ranging from zero till the indentation depth reaches 3000nm and then the specimen is unloaded. As the load is applied, the depth of penetration is measured. The area of contact at full load is determined by the depth of the Impression and the known angle or radius of the indenter. The hardness is found by dividing the load by the area of contact.

Shape of the unloading curve provides a measure of elastic modulus. Load versus displacement are recorded for each sample, when indenter reaches final indentation depth Hardness and modulus value is displayed.

4. HARDNESS RESULTS AND DISCUSSION

Load applied and indentation depth is the output of the experiments conducted. Also equipment displays hardness and reduced modulus values directly. Load is gradually applied till the indentation depth reaches 3000nm and then the specimen is unloaded.

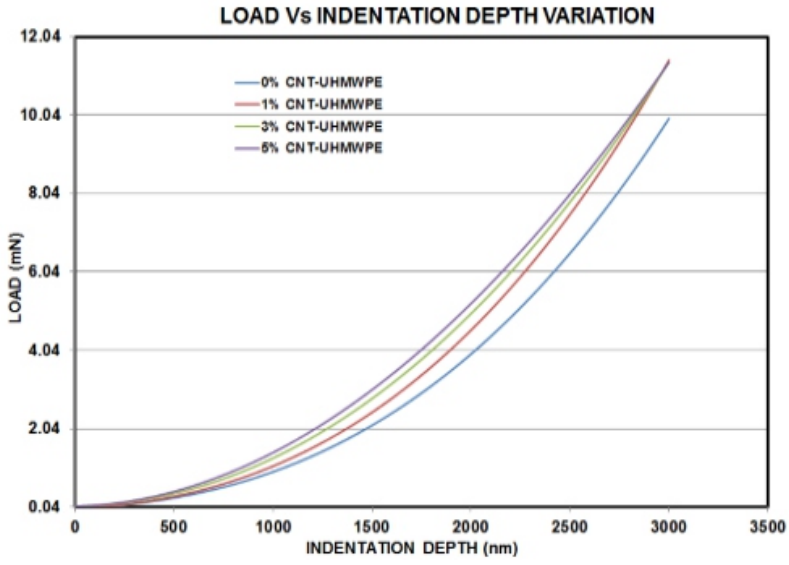

Figure 4. Load Vs Indentation Depth

Indentation depth variation with respect to load is shown in figure 4. From the figure it is observed that, the ascent of curve due to load application is increased with increase in MWCNT weight percentage in the polymer. This behaviour indicates that, to have same indentation depth the load required is more when MWCNT concentration is high in the polymer composite. Also it justify that the Ultra high molecular weight polyethylene material is hardened when the filler material MWCNT is added. To have indentation depth 2000nm, the load required for pure Ultra high molecular weight polyethylene is 6.5mN and with 1%, 3% and 5% filler addition the load required to have same indentation depth increases to 7.5mN, 7.82mN and 8mN

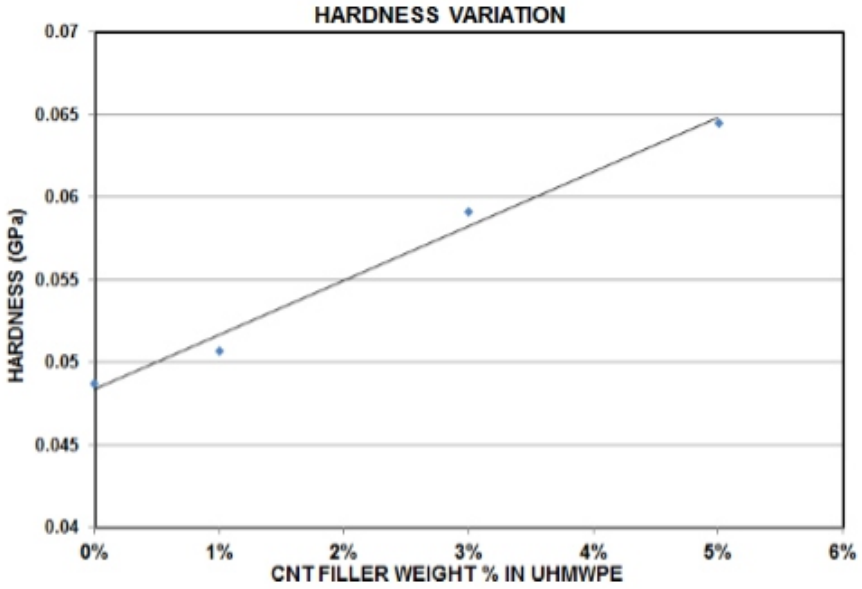

Figure 5.Hardness variation with respect to filler variation

Figure 5 shows Hardness variation with respect to filler material weight percentage. Hardness value quoted by test equipment is averaged to get single hardness property for respective material. It is observed that hardness value increases linearly with increase in carbon nano tube weight percentage in pure UHMWPE material. For pure UHMWPE material it is observed that hardness value is 48.7 MPa but when 5% carbon nano tube is added to polymer, hardness increased to 64.5 MPa.

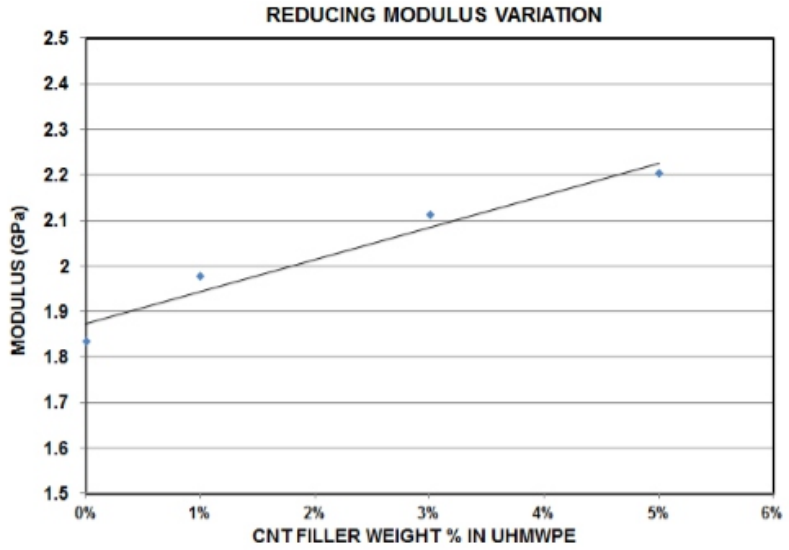

Figure 6. Reducing Modulus Variation

Figure 6 shows Modulus variation with respect to filler material weight percentage. It is observed that modulus value increases linearly with increase in carbon nano tube weight percentage in pure UHMWPE material. For pure UHMWPE material it is observed that hardness value is 1.8 GPa but when 5% carbon nano tube is added to polymer, modulus increased to 2.2 Gpa.

MWCNT addition to UHMWPE will increase the toughness of the composite material which in turn makes material harder which is evident from discussed results

VALIDATION

The experimental results are validated using the Oliver and Pharr analytical model. The indentation load (P) with displacement (h) data obtained during one full cycle of loading and unloading. The important parameter in the model is S, which has the dimensions of force per unit distance and is known as elastic contact stiffness. Hardness (H) of material and Modulus(Er) property is evaluated using this parameter. The fundamental relations from which H and E are determined are:

$$H = P/A \quad \text{..... (1)}$$

Where P is the load in milli N and A is the projected contact area at the corresponding load, and:

$$E_r = \frac{\sqrt{\pi}}{2\beta}\frac{S}{\sqrt{A}} \quad \text{..... (2)}$$

Where Er is the reduced elastic modulus and β is a constant that depends on the geometry of the indenter.

Using equation-1 hardness value for all samples are evaluated and plotted against experimental results as shown in Figure 7.The deviation in validation is approximately 13%. Tabel-1 shows hardness values obtained from experimental and analytical calculation.

Material	Hardness (Mpa)		Deviation (%)
	Experimental	Analytical	
Pure UHMWPE	48.68	42.31	13
1% MWCNT	50.75	44.55	12
3% MWCNT	59.17	50.90	14
5% MWCNT	64.47	55.26	14

Table 1.Hardness values and deviation

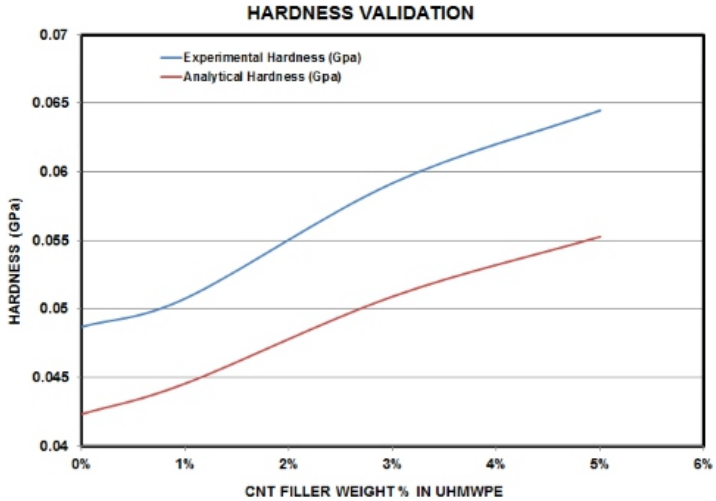

Figure 7.Hardness validation

Similarly reduced modulus is evaluated analytically for 5% CNT composite which is compared against experimental results as shown in Figure 8. The deviation in validation observed is 25%. Though the deviation is observed in validation the deviation remains constant for all conditions.

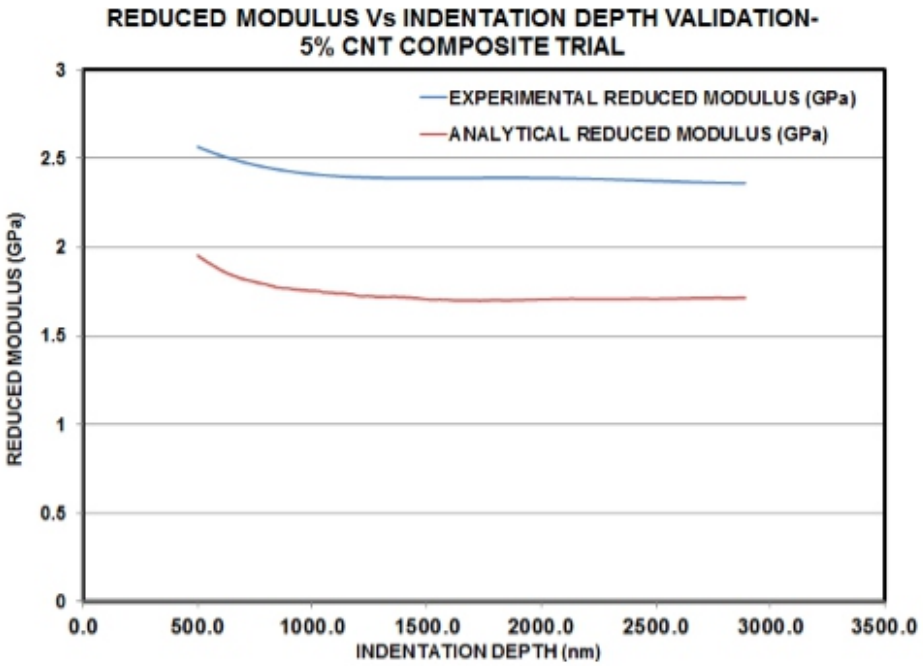

Figure 8.Reduced Modulus validation

5. CREEPTEST

Creep test is performed using Keysight Nano indenter G200 make. Testing parameter and indenter type considered is similar to what used in hardness testing. To simulate creep behavior, the sample is made to undergo constant loading for standard duration once it reaches stated indentation depth. Testing procedure as explained below.

Test is started by applying load in milli Newton ranging from zero till the indentation depth reaches 2300nm and then the specimen is continued to load at constant value of load for 10mins. Load versus displacement are recorded for each sample. When load is held constant for 10 mins, displacements are tabulated to obtain creep displacement with respect to time. Also creep strain percentage is evaluated using initial indentation depth and indentation depth after 10mins of constant loading. These creep properties are compared with all four configuration of materials.

6. CREEPRESULTS AND DISCUSSION

Load applied and indentation depth is the output of the experiments conducted. Using this data creep displacement with respect to time is extracted.

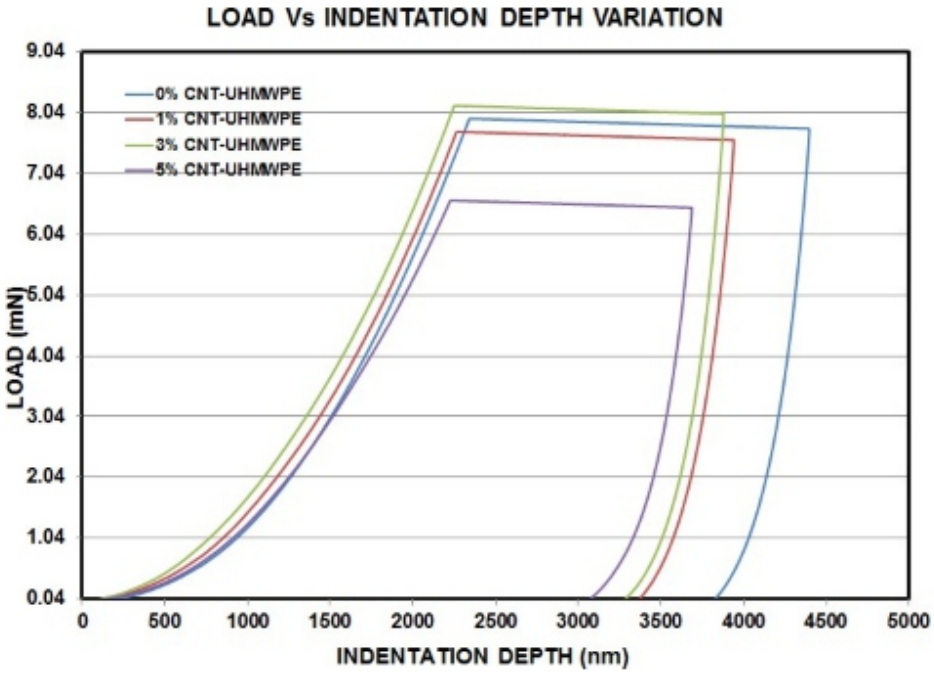

Figure 9.Load Vs Indentation

Figure 9 shows load variation with respect to indentation depth for all the materials which is the output of the experiments. Compared to hardness test, here after loading the sample up to predefined indentation depth the samples undergoes constant load for constant defined time that is 10mins and then unloaded. From the results it is observed that the creep displacement after 10mins is not same for all the materials. By appearance pure UHMWPE experiences more creep displacement and 5% MWCNT reinforced polymer composite experiences least creep displacement

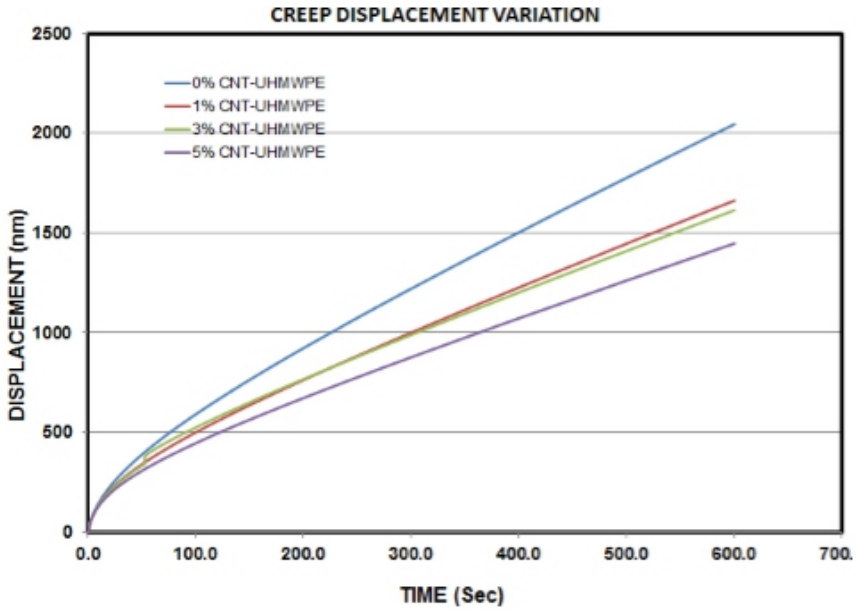

Figure 10.Creep Displacement wrt time

Figure 10 shows creep displacement variation with respect to time for all the materials. The displacement experienced for constant load condition at fixed time period is used to extract creep displacement variation with respect to time. It is observed that creep displacement increases as the time

increases. The point at which indentation depth 2300nm is reached and after that the load is kept constant is considered as zero time zero displacement. To quantify after 10mins, pure UHMWPE material experiences creep displacement of 2045nm. Whereas composite material with 1%, 3% and 5% weight percentage of MWCNT experiences 1662nm, 1613nm and 1446nm of creep displacement.

Figure 11 shows creep strain variation with respect to time for all the materials. To evaluate creep strain indentation depth of 2300nm is considered as actual penetration and indentation after 10mins of hold time is considered as change in penetration. It is observed that creep strain reduces linearly as MWCNT weight percentage increases in UHMWPE composite material.

The creep resistance of material increases as Carbon Nano tube is reinforced with Ultra high molecular weight polyethylene. It can be studied that creep strain value decreased from 87% for pure polymer to72.8% for 1 Wt. % composite samples which lead to 14% decrease. The creep strain of 3 Wt. % and 5 Wt. % composite samples decreases to 71% and 64%.

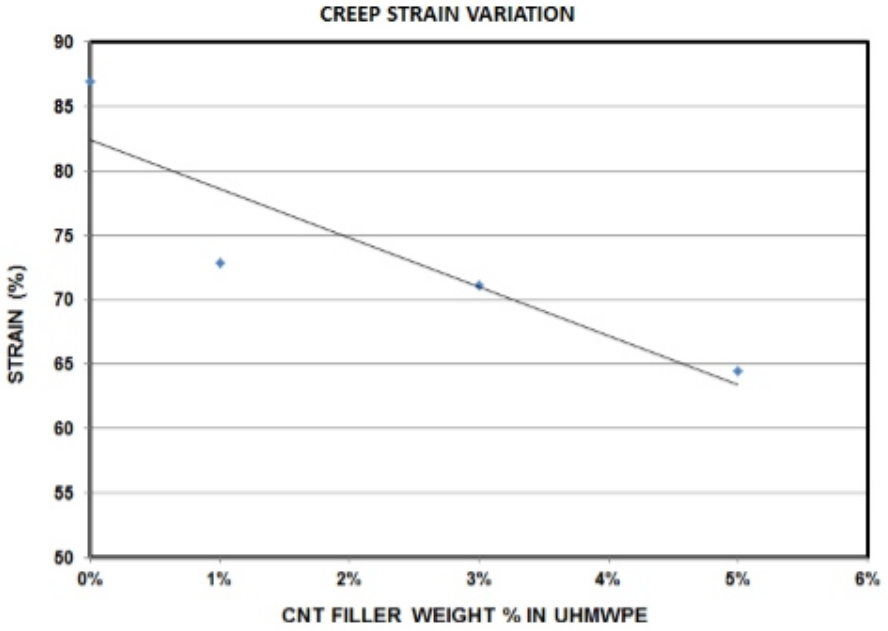

Figure 11.Creep strain variation

From the results it is understood that creep resistance increases as filler material MWCNT is added to pure UHMWPE material. The MWCNT has very good toughness property which in turn helps in enhancing the hardness and creep resistance property.

7. CONCLUSION

In this article the Ultra high molecular weight polyethylene and the Ultra high molecular weight polyethylene composites are successfully fabricated using compression molding technique and the effect of Carbon nano tube weight percentage is studied. The conclusions are as follows:

1. CNT reinforced composites shows improved creep properties compared to polymer alone material. With 1%, 3% and 5% CNT addition to polymer the creep displacement decreased by 18%, 21% and 29%
2. CNT reinforced composites shows improved surface hardness value compared polymer alone material. With 1%, 3% and 5% CNT addition to polymer the hardness value increased by 4%, 18% and 25%

3. Elastic modulus increases as carbon nano tube added to polymer alone material. With 1%, 3% and 5% CNT addition to polymer the modulus value increased by 7%, 13% and 16.7%
4. Using analytical model, Experimental results for Hardness value are validated with 13% variation and Modulus value are validated with 24 % variation

REFERENCES

[1] S. Ramakrishna, J. Mayer, E.Wintermantel, Kam W. Leong, "Biomedical application of Polymer composite material: a review", Composite Science and Technology 61, pp. 1189-1224, 2001

[2] George Matsoukas et al: Jour of Biomechanical Engineering, ASME Vol 131, (2009).

[3] Shirong Ge , Xueqin Kang, Yujie Zhao, "One-year biodegradation study of UHMWPE as artificial joint materials: Variation of chemical structure and effect on friction and wear behavior", Wear, Volume 271, Issues 9–10, Pages 2354– 2363, 2011

[4] J. Zhou and F. Yan, "Improvement of tribological behavior of UHMWPE by incorporation of Poly(phenyl p-hydroxyzonate)", J. Appl. Polym, Sci. 96,2336 (2005)

[5] V.A. Gonzlez-More, M. Hoffmann, R. Stroosnijder, and F. J. Gil, "Wear test in Hip joint simulator of different Co- Cr-Mo counterfaces on UHMWPE", Polymer material scienece Engineering C29, 153, 2009

[6] K. Chen, D. Zhang, and S. Wang, "Start-up friction properties of poly (vinyl alcohol)/ nano-hydroxyapatite/ silk composite hydrogel", Material Express 3, 265, 2013

[7] H. Liu, S. Ge, S. Cao and S. Wang, Comparison of wear debris generated from UHMWPE in vivo and in artificial joint simulator , Wear 271, 647, 2011

[8] P. S. Rama Sreekanth, N. Naresh Kumar, S. Arun and S. Kanagaraj, "Effect of multi-walled carbon nanotubes reinforcement and gamma irradiation on viscoelastic properties of ultra-high molecular weight polyethylene" Materials Research Innovations, Volume 00, 2015

[9] Silvia Suñer, Catherine L Bladen , Nicholas Gowland, Joanne L Tipper, NazaninEmami, "Investigation of Wear and Wear Particles from a UHMWPE/Multi-Walled Carbon Nanotube Nanocomposite for Total Joint Replacements", Wear 317, 163-169, 2015

[10] S. Kanagaraj, A. Fonseca, R.M. Guedes, M.S.A. Oliveira, J.A.O. Simoes, "Thermo-mechanical behavior of ultrahigh molecular weight Polyethylene-carbon nanotubes composites under different cooling techniques", Volume 2014.

Modulus of Elasticity for Steel Fibre Reinforced Recycle Aggregate Concrete

C. Sashidhar*, .Venkata Subbareddy* N. Venkata Ramana ****

* Research Scholar, JNTUA, Anantapur, A.P, India, PIN: 515002

** Associate Professor, UBDT College of Engineering Davangere, Karnataka (State), India (Country), PIN 577004, Email: rccramana@gmail.com

*** Professor, JNTUA College of Engineering, Anantapur, A.P, India, PIN: 515002

ABSTRACT

The paper presents the Modulus of Elasticity of recycle aggregate concrete reinforced with low strength steel fibers. In the experimental work the recycle aggregate is used in place of natural aggregate in the proportion of 0,25,50,75 and 100% with and without incorporation of steel fibers. The fibers were prepared by cutting the binding wire in required length of 50mm and the diameter was noticed as 1mm. These fibers were added to the recycle aggregate concrete mixes in the proportion of 0, 1, 1.5 and 2% by volume fraction of the cast specimens. The mixes without addition of fibers were taken as reference mixes and these are used for comparison purpose. Total 60 cubes and 60 cylinders were cast and tested to obtain compressive strength and modulus of elasticity's for various mixes. The obtained results are compared with IS code provision and earlier research works. Regression models are also deduced to suit the experimental data and checked its validity. The results found that the strengths are reducing as the percentage of recycle aggregate content increases and also observed that as the fiber content increases in the mixes the strengths are increasing.

Keywords : Compressive strength; Modulus of elasticity; Natural aggregate concrete; Recycle aggregate concrete; Regression model.

1. INTRODUCTION

Modulus of Elasticity is also known as the Young's modulus, it is a measure of the stiffness of a solid material. It is a mechanical property of linear elastic solid materials. It defines the relationship between stress (force per unit area) and strain (proportional deformation) in a material. Young's modulus is named after the 19th-century British scientist Thomas Young. However, the concept was developed in 1727 by Leonhard Euler, and the first experiments that used the concept of Young's modulus in its current form were performed by the Italian scientist Giordano Riccati in 1782, pre-dating Young's work by 25 years. A solid material will deform when a load is applied to it. If it returns to its original shape after the load is removed, this is called elastic deformation. In the range where the ratio between load and deformation remains constant, the stress-strain curve is linear. Not many materials are linear and elastic beyond a small amount of deformation. A stiff material needs more force to deform compared to a soft material, and an infinite force would be needed to deform a perfectly rigid material, implying that it would have an infinite Young's modulus. Although such a material cannot exist, a material with a very high Young's modulus can be approximated as rigid. The Young's modulus enables the calculation of the change in the dimension of a bar made of an isotropic elastic material under tensile or compressive loads. For instance, it predicts how much a material sample extends under tension or shortens under compression. The Young's modulus directly applies to cases of uni-axial stress, that is tensile or compressive stress in one direction and no stress in the other directions. The present experimental work was focused to evaluate the young's modulus of recycle aggregate concrete with and without addition of

steel fibres. For this the cylinders were cast and tested in the laboratory by applying uni-axial stress. In addition to the cylinders, the cubes were cast and tested; the compressive strength results were used during deducing of the regression models. Before going to detailed experimental work a resent past literature is presented below to know the scenario.

Shen Dejian and LU Xilm [1] presented the relationship between compressive strength, modulus, peak strain and failure type of micro concrete under compression. V.S.Sethuraman and K.Suguna [2] conducted the experimental study to evaluate modulus of elasticity of M60 grade concrete using standard cylinder specimens, tested with compress meter under axial compression, in their study it is observed that the stress-strain behavior exhibits non-linear variation and from which the initial tangent modulus is plotted to arrive at modulus of elasticity values. IsamuYoshitake, Farshad Rajabipour, YoichiMimura and Andrew Scanlon [3] provided the results for Young smodulus of concrete and also gave the information of cracking due to restrained shrinkage and thermal construction. Byung Jae Lee, Seong-Hoon Kee, Taekeun Oh and Yun-Yong Kim [4] investigate the effect of cylinder size (150 by 300 mm and 100 by 200 mm) by using empirical equations that relate static elastic moduli and compressive strength and static and dynamic elastic moduli of concrete. Gupta Arundeb, Mandal Saroj and Gosh Somnath [5] studied the change in direct compressive strength and elastic modulus of recycled aggregate concrete in presence of fly ash (as replacement of cement). K.Krizova and R.Hela [6] studied the effect of dependencies of different composition concretes on elastic modulus values. N. Anusha and A V S Sai Kumar [7] studied the mechanical behavior of concrete in terms of modulus of elasticity with the change of aggregate size reinforced with steel fibers of different series for M30 and M50 grade concretes. U.Venkat Tilak and A.Narender Reddy [8] studied the effects of coarse aggregate on the modulus of elasticity of HPC concrete. Praful Vijay [9] studied the flexural and elastic modulus behavior of Lightweight aggregate in concrete with provision of steel fibers. The results revealed that, the concrete mix with steel fibres increases the tensile, flexural and elastic modulus properties. Dr.V.Bhaskar desai and A.Sathyam [10] studied the strength prosperities of light weight cinder aggregate cement concrete in different percentage proportions of 0, 25, 50, 75 and100 by volume of light weight aggregate concrete. The study was aimed to evaluate compressive strength, split tensile strength, modulus of elasticity, density and shear stress. K.Anbuvolan and Dr.K.Subramanian [11] presented the relationship between modulus of elasticity and modulus of rupture relationship for compressive strength of M60 concrete by incorporating the steel fibres. M.Ispir, K.D.Dalgic C.Sehgul, F.Kuran, Allki and M.A.Tasdemir [12] aimed to determine the modulus of elasticity of low strength concrete. From the literature it came to know that, no works has been carried out to estimate modulus of elasticity for recycle aggregate concrete by incorporation of low strengthsteel fibres with dosage of 1, 1.5 and 2% by volume fraction of cast specimen. In this direction an experimental study was planned to estimate modulus of elasticity for RAC mixes, the detailed test programme was presented below.

2. TEST PROGRAMME

The experimental program consists of a total of 60 cubes and 60 cylinders. The standard cubes (60 cubes) were cast and tested in the compressive testing machine to know the compressive strengths for different mixes. Among 60 cylinders, 15cylinders are without fibres and remaining 45 cylinders were cast with steel fibres of 1, 1.5 and 2% volume of specimen respectively. For each mix three specimens were cast and tested, the average of three specimens was taken as strength of mix. Each cylinder was tested in compressive testing machine and for the cylinder the longitudinal extensometer was attached to find strains. The stress stain diagram was plotted for the mixes and young's modulus was found from the graphs. For all the mixes the concrete was designed for M20 grade concrete as per ACI 211 code. The

mix proportions are presented in Table 1. From the literature is is noticed that, various mix designs were proposed for the RAC from the researchers. But among them, the ACI 211 code methodology was found to be sastifactory and effective results for the recycle aggregate concerte. Hence here in also the ACI code provisions were taken to design the mix proportions. In the Table1, the nomenclature can understand as the first three letters indicated as type of concrete, next two/three numerical values are indicated as % of replacement of natural aggregate by the recycle aggregate. The NAC mix was taken as reference mix and this can also observed as conventional concrete. The RAC mixes were provided with incorporation of steel fibres. For this experimental work the low strength steel fibers (yield strength of wire is 390 MPa) are obtained from binding wire, which was cut by shear cutter with aspect ratio as 5 (the diameter of wire is 1.0mm and length is 50mm). The steel fibres were mixed in the concrete mixes and care was taken to avoid balling effect during mixing of concrete.

Table 1: Mix proportions of concrete (Kg/m^3)

		Average compressive stress (MPa)			
S.No	**Nomenclature**	**0% fibre**	**1% fibre**	**1.5% fibre**	**2% fibre**
1	NAC-0-0	33.33	35.68	38.67	42.43
2	RAC-25-0	32.4	34.8	37.68	41.46
3	RAC-50-0	31.68	33.8	36.57	40.4
4	RAC-75-0	30.8	33.02	35.77	39.33
5	RAC-100-0	29.3	31.42	34.04	37.42

3. Casting

The standard cubes and cylinders were cast in steel moulds with inner dimensions of 150x150x150 for cubes and 150mm dia and 300mm height for cylinders. All the materials are weighed as per mix design and kept a side separately. The cement, sand, coarse aggregate, fibres and recycle aggregate were mixed thoroughly till to reach uniformity to the concrete mix. For all test specimens, moulds were kept on table vibrator and the concrete was poured into the moulds and the compaction was adopted by mechanical vibrator. The moulds were removed after twenty four hours and the specimens were de-moulded and were exposed to water bath for 28 days in curing pond. After curing the specimens in water for a period of 28 days, the specimens were taken out and allow drying under shade. Three cubes and cylinders were cast for each mix.

4. Testing

Compression test on cubes was conducted with 2000 kN capacity compression testing machine. The machine has a least count of 1kN. The cube was placed in the compression testing machine and the load on the cube is applied at a constant rate till to failure of the specimen and the corresponding load is noted as ultimate load. Then cube compressive strength of the concrete mix is computed by using standard formula and the obtained values are presented in next section. The cylinder specimens were tested in the laboratory to evaluate the young's modulus for various mixes. The modulus of elasticity is determined using the longitudinal compression meter attached to the specimen as shown in figure 1. The modulus of elasticity is determined by subjecting the cylindrical specimen to axial compression and measuring the deformation by means of a dial gauge fixed to the longitudinal compression meter at regular intervals. The load on the cylinder is applied at a constant rate up to the failure of the specimen cylinder. Dial gauge reading divided by gauge length will give the strain and load applied divided by area of cross section will give the stress. A series of readings are taken and the stress-strain relationship is developed. Modulus of elasticity of steel fiber reinforced RAC is calculated as its initial tangent modulus. The various stress–strain responses obtained are presented in the next section.

Figure 1: Test set up for cylinder

5. TEST RESULTS AND DISCUSSION

5.1 Compressive Strength of Concrete

The results of cube compressive strength made with natural aggregate concrete and recycle aggregate concrete for 28 days curing are presented in Table 2. For RAC25 to RAC100 the compressive strengths are decreasing form 2.7 to 12% when compared with reference or natural aggregate concrete. Initially the concrete was designed for M20 grade concrete. The various mixes with RAC was shown from 33.33 to 29.3MPa, from this it is noticed that even the RAC100 mix showing design strength value. Hence it may conclude that the mix with RAC100 is also acceptable to concrete works. Etxeberria et al,[13] and Santos et al [14] has been reported that the 28 days compressive strength for RAC100 decreased about 20 to 25% , when compared with conventional concrete. In the present work the compressive strength for RAC100 was decreased by 12% only. The different % of decrease in strengths may be due to properties of aggregate and adhere of cement mortar variation for the surface of the aggregate. The RAC mixes with fibres (1, 1.5 and 2%) also showing the decreasing in compressive strengths about 2.3 to 12%. The strength is differing for various dosages of fibres, and from table 2 it is observed that as the % of fibre increases for the mix, the compressive strengths are increasing. As per the rule of mixtures the strengths may increase as% of steel fibres are increases for the mixes. The fibres are act as energy absorbers and also act as crack arresters. During the experimentation for 2% fibre cubes, the failure pattern is differ when compared to conventional concrete. Few thin cracks were noticed for the cube of containing fibres and this behaviour was not seen for cubes with no fibres. Dimensional stability was more for higher dosage fibres even at the stage of ultimate failure load. In the present experimental work the compressive strength results can be used to make the relation with modulus of elasticity, this can be discussed in the next section.

Table 2: Compressive strength of RAC concrete with and without fibres at 28 days

		Average compressive stress (MPa)			
S.No	**Nomenclature**	**0% fibre**	**1% fibre**	**1.5% fibre**	**2% fibre**
1	NAC-0-0	33.33	35.68	38.67	42.43
2	RAC-25-0	32.4	34.8	37.68	41.46
3	RAC-50-0	31.68	33.8	36.57	40.4
4	RAC-75-0	30.8	33.02	35.77	39.33
5	RAC-100-0	29.3	31.42	34.04	37.42

5.2 Modulus of Elasticity (ME)

The modulus of elasticity of a material in compression is a fundamental property that is needed for modelling its mechanical behaviour and for evaluation of stiffness criteria. Due to the high volume fraction of steel fibers, the concrete has not only very ductile compressive stress-strain behaviour, but also has ductile flexural, tensile and cyclic behaviour. There are a vast number of potential applications for such a composite particularly in earthquake and impact resistant structures. For safe and efficient use, the stress - strain response of the composite should be known, with the peak strength and the modulus of elasticity being two of the most important parameters of this response. The increasing application of damage mechanics to civil engineering composites calls for the knowledge of the modulus of elasticity and its deterioration or damage with loading history. Thus, there is need to generate experimental data related to the elastic modulus of steel reinforced RAC.

The stress strain curves for various mixes are presented in figure 2 to 5. From this curves the initial tangent modulus was drawn and corresponding slopes of the curve were taken as modulus of elasticity corresponding mixes. The obtained moduli of elasticity (ME) values are presented in Table 3. From this table it is observed that, mixes with 0% fibres for various replacements of recycle aggregates was varying about 2.53x104 to 2.71x104MPa. The percentage of decrease in ME is about 1.85 to 6.65% for RAC25 to RAC100, when compared with natural aggregate concrete respectively. This type of results are observed by the Kou and Poon [15], in their study the decrease is about 10% for RAC100 aggregate concrete over conventional concrete. But in the present experimental work the decrease for RAC100 noticed as 6.65% over reference mix. So in general it may conclude that, as percentage of recycle aggregate content increases the modulus of elasticity is decreasing. This may due to stiffness of mortar, concrete porosity and aggregate cement paste bonding. For mixes with addition of fibres of 1, 1.5 and 2% the ME values are varying 2.57 x104 to 3.08 x104, 2.61 x104 to 3.23 x104 and 2.72 x104 to 3.36 x104 MPa respectively. The % of decrease for 1% mix RAC25 to RAC100 is about 7 to 16%, when compared with reference mix of 1% fibre. In the similar way for 1.5% and 2% of RAC25 to RAC100 is about 6 to 10% and 5 to 10% respectively over corresponding mix of fibre reinforced natural aggregate concrete. In all the mixes as the % of RA content increases the ME values are decreasing. At the same time as the % of steel fibres content increases for the same mix the modulus of elasticity values are increasing (this can noticed from Table 3).

Table 3: Modulus of Elasticity for Various Mixes

	0% Fibre	1% Fibre	1.5% Fibre	2% Fibre
Nomenclature	**10^4 MPa**			
NAC	2.71	3.08	3.23	3.36
RAC25	2.66	2.86	3.03	3.17
RAC50	2.62	2.67	2.84	3
RAC75	2.58	2.62	2.68	2.85
RAC100	2.53	2.57	2.61	2.72

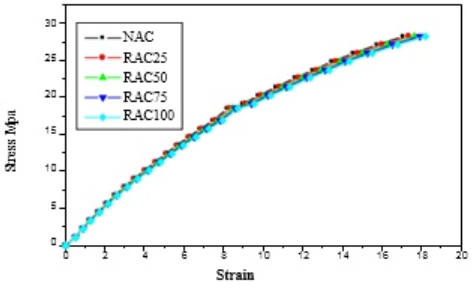

Figure 2: Stress – Strain response of 0% of Fibre

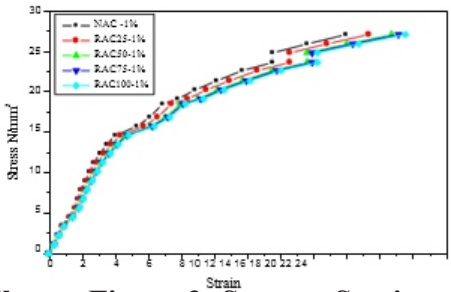

Figure 3: Stress – Strain response of 1% of Fibre

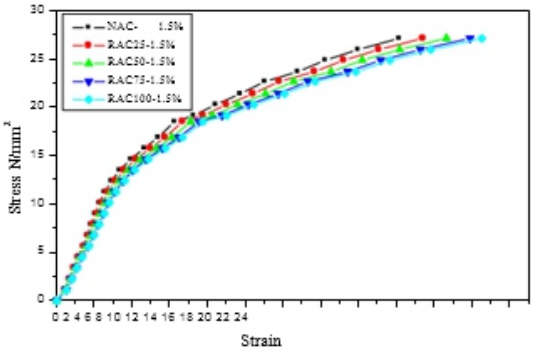

Figure 4: Stress – Strain response of 1.5% of Fibre

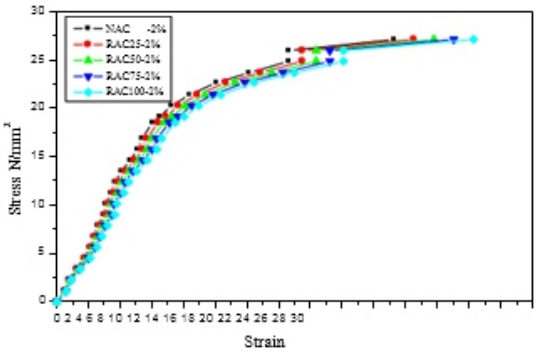

Figure 5: Stress – Strain response of 2% of Fibre

The authors would like test the modulus of elasticity values with the earlier research works and also with IS 456 code provision. Though the IS formula specified for conventional concrete, here in it is testing for the suitability of the experimental results. Earlier researchers Ravindrarajah and Tam [16], Dhir et.al [17], Corinaldesi et.al [18] and Xiao et.al [19] has been provided formulas to find Youngs modulus for RAC concrete. At present, those are tested in Table 4 as suitability of equation for steel fibre reinforced recycle aggregate concrete. In addition to the table for better understanding the behaviour of RAC, graphs are also drawn and are depicted in figure 6 to 9. For 0% fibre mix the modulus of elasticity values are over estimated by the IS code and underestimated by the earlier researchers (figure 6). For RAC with 1, 1.5 and 2% fibres the Modulus of elasticity is more for natural aggregate concrete but for 25 to 100% RA, the values are overestimate by The IS Code and underestimated by the earlier works (figure 7, 8 and 9). In order to estimate reasonably the authors are planned to develop regression model as the model be a function of compressive strength of mix, %RAC and % of Steel fibres.

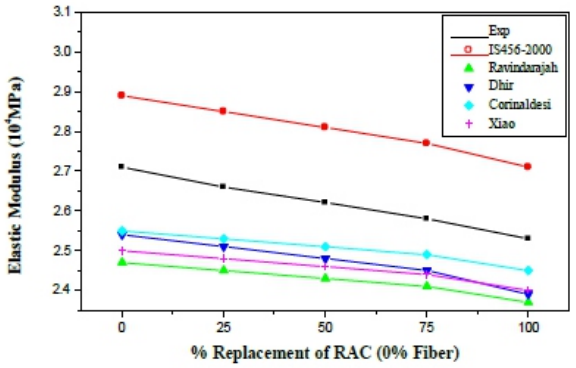

Fig 6:Elastic modulus vs % of RAC (0.0% fibre)

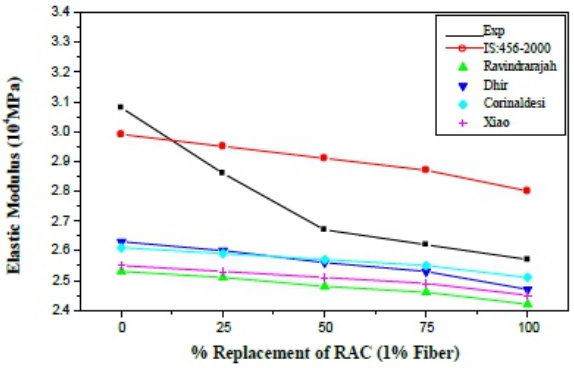

Fig 7:Elastic modulus vs % of RAC (1.0% fibre)

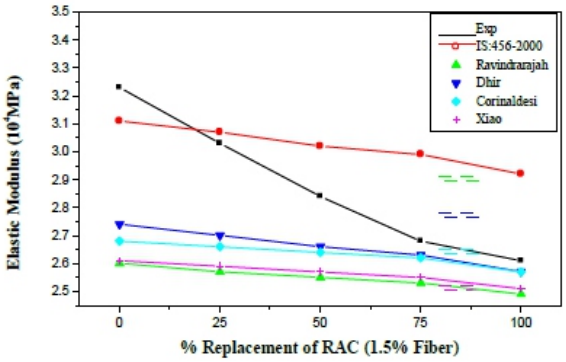

Fig 8:Elastic modulus vs % of RAC (1.5% fibre

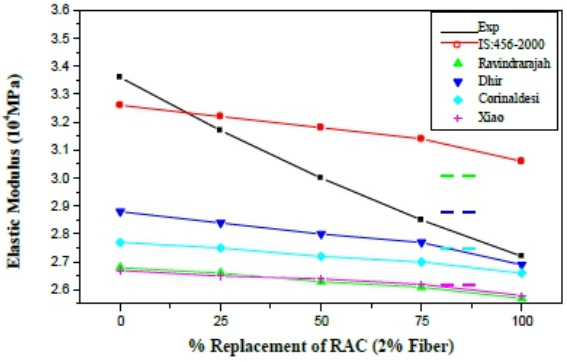

Fig 9:Elastic modulus vs % of RAC (2.0% fibre)

Table 4: Modulus of elasticity for RAC concrete

Sl. No	Nomenclature	Experimental	As per IS code E=5000?fcu	Ravindrarajah and Tam(1985) E=7770x $(fcu)^{0.33}$	Dhir et al.(1999) E=370x fcu+131 00	Corinaldesi et al.(2011) E=18.2[((0.83*fcu)/10) $^{1/3}$]	Xiao et al.(2006), $E=10^5/(2.8+(40.1/fcu))$
		10^4 N/mm^2					
0% of Fibres							
1	NAC0	2.71	2.89	2.47	2.54	25.55	2.5
2	RAC25	2.66	2.85	2.45	2.51	25.31	2.48
3	RAC50	2.62	2.81	2.43	2.48	25.12	2.46
4	RAC75	2.58	2.77	2.41	2.45	24.89	2.44
5	RAC100	2.53	2.71	2.37	2.39	24.47	2.4
1.0% of Fibres							
6	NAC0	3.08	2.99	2.53	2.63	26.14	2.55
7	RAC25	2.88	2.95	2.51	2.6	25.92	2.53
8	RAC50	2.67	2.91	2.48	2.56	25.67	2.51
9	RAC75	2.62	2.87	2.46	2.53	25.47	2.49
10	RAC100	2.57	2.8	2.42	2.47	25.05	2.45
	1.5% of Fibres						
11	NAC0	3.23	3.11	2.6	2.74	26.85	2.61
12	RAC25	3.03	3.07	2.57	2.7	26.62	2.59
13	RAC50	2.84	3.02	2.55	2.66	26.35	2.57
14	RAC75	2.68	2.99	2.53	2.63	26.16	2.55
15	RAC100	2.61	2.92	2.49	2.57	25.73	2.51
2.0% of Fibres							
16	NAC0	3.36	3.26	2.68	2.88	27.69	2.67
17	RAC25	3.17	3.22	2.66	2.84	27.48	2.65
18	RAC50	3	3.18	2.63	2.8	27.24	2.64
19	RAC75	2.85	3.14	2.61	2.77	27	2.62
20	RAC100	2.72	3.06	2.57	2.69	26.55	2.58

5.2 Regression Model for Modulus of Elasticity of RAC

The Indian standard code IS 456 – 2000 provided a square root function to estimate the modulus of elasticity of concrete as $E = 5000\sqrt{fck}$,

Where,
E is the modulus of elasticity in N/mm2 and
fck is cube compressive strength of 28 days in MPa .

In similar manner, regression model has been developed as square root function of characteristic compressive strength along with other variables of %of RAC & % of fibre.

Based on regression analysis of the results of present investigation, the following model is recommended.

$$E = 0.38181+0.43753(\sqrt{fck}) - 0.03441(\sqrt{RAC}) + 0.04066(\%\ of\ fibre)$$

Where,
fck = cube compressive strength of 28 days in Mpa.
RAC= Recycle Aggregate Concrete.

E= Youngs modulus in MPa

The validity of the equation is depicted in Table 5 and in Figure 10. In general for most of the cases the regression models are able to predict the modulus of elasticity reasonably well. Here also the maximum difference observed is about 10%. Hence it is recommended that the above model can be used for predicting the modulus of elasticity approximately for various mixes of RAC (with and without fibres).

Table 5: Performance of Regression Model (RM)

Nomiclature	0%Fibre		1%Fibre		1.5%Fibre		2%Fibre	
	10^4 N/mm^2							
	EXP	RM	EXP	RM	EXP	RM	EXP	RM
NAC	2.71	2.91	3.08	3.04	3.23	3.16	3.36	3.31
RAC25	2.66	2.7	2.88	2.83	3.03	2.96	3.17	3.11
RAC50	2.62	2.6	2.67	2.72	2.84	2.85	3	3
RAC75	2.58	2.51	2.62	2.64	2.68	2.76	2.85	2.91
RAC100	2.53	2.41	2.57	2.53	2.61	2.65	2.74	2.8

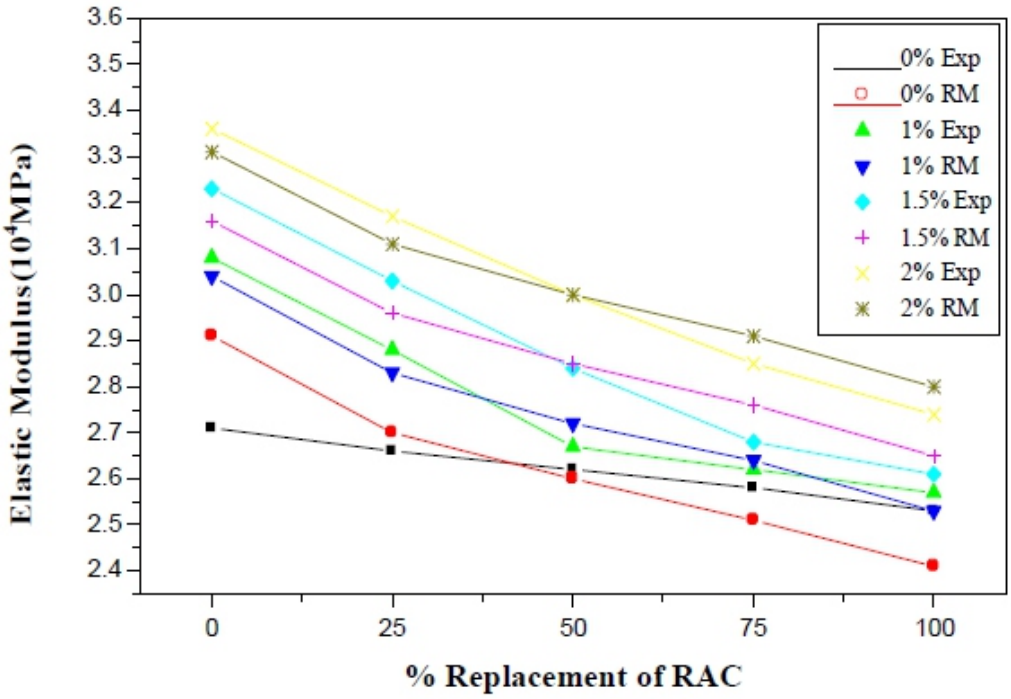

Fig 10: Performance of Regression model

6. CONCLUSIONS

The following conclusions were drawn from the experimental work.

1. The compressive strength is decreasing for the RAC mixes as the % of recycle aggregate increased in the mixes. The compressive strength is varying about 2.3 to 12% for RAC mixes when compared to conventional concrete.
2. The moduli of elasticity also decreasing as the % of recycle aggregate content increases in the mixes. The modulus of elasticity for RAC concrete (with out fibres) is is decreased by 1.85 to 6.65% when compared with reference mix. The modulus of elasticity for RAC with fibres (1 to 2%) was decreased from 5 to 10% over reference concrete containing corresponding dosage of fibres.

3. As the %of steel fibres increases for the RAC mixes the compressive strength and modulus of elasticity is increasing.
4. The validity of the equation proposed by the earlier researchers are checked and found as those are under estimating the experimental results.
5. A regression model has been developed to evaluate the modulus of elasticity with the functions of compressive strength, % of RAC and % of steel fibres.
6. Load deflection curves for various mixes are plotted from those it is observed that the stiffness is marginally varying.

REFERENCES

[1] Shen Dejian and LU Xilin,"Experimental Study on Dynamic Compressive Properties Of Microconcrete Under Different Strain Rate," 14th World Conference on Earthquake Engineering,October, Beijing, China12-17, 2008.

[2] V.S.Sethuraman and K.Suguna, "Computation of Modulus of Elasticity of High Strength Concrete using Silica Fume," Asian Journal of Applied Sciences, Volume 04 – Issue 01, February 2016.

[3] Isamu Yoshitake, Farshad Rajabipour, Yoichi Mimura and Andrew Scanlon, "A Prediction Method of Tensile Young's Modulus of Concrete at Early Age," Hindawi Publishing Corporation Advance in Civil Engineering, Volume 2012, Article ID 391214.

[4] Byung Jae Lee, Seong-Hoon Kee, Taekeun Oh and Yun-Yong Kim, "Effect of Cylinder Size on the Modulus of Elasticity and Compressive Strength of Concrete from Static and Dynamic Tests," Hindawi Publishing Corporation Advance in Civil Engineering, Volume 2015, Article ID 580638.

[5]Gupta Arundeb, Mandal Saroj and Ghosh Somnath, "Direct compressive strength and Elastic modulus of recycle aggregate concrete," Inernational Journal Of Civil And Structural Engineering, Volume 2, No 1, 2011.

[6]K.Krizova and R.Hela, "Evaluation of Static Modulus of Elasticity Depending on Concrete Compressive Strength," World Academy of Sciences, Engineering and Technology, International Journal of Civil, Environmental, Structural, Construction and Architectural Engineering Vol;9, No:5, 2015.

[7]N.Anusha and AVS.Sai Kumar, "Experimental stud of Modulus of Elasticity due to change in steel fiber reinforced concrete (SFRC) and size of aggregates," International Journal of Scientific & Engineering Research, Volume 6, Issue 7, July-2015.

[8]U.Venkat Tilak and A.Narender Reddy, "Effect of Different Percentage Replacement of Weathered Aggregate in Place of Normal Aggregate on Young's Modulus of Concrete to Produce High strength and Flexible/Ductile Concrete for use in Railway Concrete Sleepers," SSRG International Journal of Civil Engineering (SSRG-IJCE) – Volume 2, Issue 11, November 2015.

[9]Praful Vijay, "Flexural and Elastic Modulus Behavior of Lightweight Aggregate in Concrete and Structures," International Journal of Emerging Technology and Advanced Engineering, Volume 5, Issue 2, February 2015.

[10]Dr.V.Bhaskar desai and A.Sathyam, "Some Studies on Strength Properties of Light Weight Cinder Aggregate Concrete," International Journal of Scientific and Research Publications, Volume 4, Issue 2, February 2014

[11]K.Anbuvelan and Dr.K.Subramanian, "Exprimental investigation on Elastic Properties of Concrete Containing Steel fiber," International Journal of Engineering and Technology.

[12] M.Ispir, K.D.Dalgic, C.Sengul, F.Kuran, A.Ilki and M.A.Tasdemir, "Modulus of elasticity of low strength concrete," 9th International Congress on Advance in Civil Engineering, 27-30, September 2010.

[13]Etxeberra M, Mari A, Vazquez E,"Recycle aggregate concrete as structural material", Mater Struct, 40(5),529- 541,2007

[14]Santos JR,Branco F de Brito J,"Mechanical properties of concrete with coarse recycled concrete aggregates Suitable buildings 2002:, Conference proceedings Oslo,2002

[15]Kou SC, Poon Ch, Chan D, "Influence of fly ash as a cement addition on the hardened properties of recycle aggregate concrete", Mat and Struct, 41(7),1191-1201,2008

[16]Ravindrarajah RS, Tam TC,"Properties of concrete made with crushed concrete as coarse aggregate", Maga Concr Res, 37(130),29-38,1985

[17]Dhir Rk, Limbachiya MC, Leelawar T, "Suitability of recycle aggregate concrete for use in BS5328 designated mixies", Structural Buildings,134(4),257-274,1999.

[18]Coeinaldesi V, "Structural concrete prepared with coarse aggregate for investigation to design advances in civil engineering, Advances in civil engineering,Vol 2011, Article ID283984, 6,2011

[19]Xiao JZ, Li JB, Zhang C,"Mechanical properties of recycle aggregate concrete under uni axial loading", Cem Concr Res, 25(6),1187-1194,2006

Reliability Assessment of Flat Slab Building using Pushover Analysis

Nikhil P[1,a], Rekha B[2,b]

[1]P G Student, School of Civil Engineering, Reva University, Bengaluru, India

[2]Assistant professor, School of Civil Engineering, Reva University, Bengaluru, India

ABSTRACT

Concrete is said to be workable, durable but it is never mentioned as reliable only because of the uncertainties that are present in it. These uncertainties can be measured by performing reliability analysis. American Concrete Institute (ACI) code classifies the state of structure based on reliability index value which is not specified in Indian codes. This study was to compare the seismic response and reliability index by taking base shear values of flat slab and conventional beam slab buildings using non-linear static analysis. It is a method to calculate seismic performance point along with the failure pattern. Both the buildings – flat slab and conventional beam slab – were analysed by considering the uncertainties in material properties, geometric properties and loads applied. Pushover analysis was carried out for different random values that were created by using Monte Carlo Simulation method to get the reliability index. The non-linear static analysis was carried out in SAP 2000 and the results were plotted. The study reveals that the flat slab system has increased failure rate compared to the beam slab system with higher hinge formations because of randomness and hence reliability analysis can be mandated as an industrial practice. The current study not only reveals the comparative advantage but also fills the gaps in failure pattern study, which is existing in this research fraternity.

Key words:- Reliability Analysis, Vulnerability Analysis, Failure pattern study, Pushover analysis, Flat Slab System

INTRODUCTION

With the tremendous growth instructural design aspects there is a desperate need in knowing the type of slab system that is to be adopted based on the consideration of seismic loads. From past few years, Performance Based Seismic Design came into existence where in, it fills the gap between linear analysis methods and the dynamic Non-Linear behaviour of structures. Seismic vulnerability can be stated as the tendency of structure to damage during the ground motion. It is a relationship between the ground motion and intensity of structural damage state .In this paper, a comparative study on Seismic performance of Flat slab system over a conventional Beam slab system was carried out for all the seismic zones by using Non-linear Static Pushover analysis as a tool which gives progressive collapse of the structure along with the plastic deformation of hinges. Concrete structures possess various number of uncertainties which are not considered in our design concepts and hence to understand the effect of these uncertainties in seismic performance, Reliability Analysis was carried out. This paper observed that there is a dearth of literature on the seismic behaviour of flat slab system and the objective of the study is to overcome this gap.

Da Gang Lu [2008], made a study on global reliability along with the combination of random pushover analysis, point estimation method and MCS over a RC frame structure to get the seismic performance and found out a new semi-analytical approach, which comprises pointestimation method, pushover analysis and FORM. By applying the proposed methodology in reinforcedconcrete frame buildings,

some changing rules of global seismic reliability of the structure with COV of totalseismic action and correlation coefficient of storey-level seismic forces were obtained.

Hardik[2015],carried out a study on pushover analysis of RC frame with floating column and soft story in different seismic zones by varying the stories respectively using SAP 2000. As it concluded that the base shear and displacement values increased as the number of stories and zone increased. The displacement value increases when floating columns were placed.

The study on literatures has shown that there is a very less of information about the seismic behaviour of flat slab system over a beam slab system in different seismic zones and also the effect of randomness that is present in concrete when analysed by pushover analysis.

System Development

The simulation study was performed in 3 phases,

1. Modelling of slab systems using SAP 2000:

The actual behaviour of the structure cannot be prototyped and analyzed due to the time and economic factors, and hencea tool based classical approach is implemented using SAP 2000. Conventional beam slab and flat slab with drop structures were modelled in SAP 2000 by keeping the same geometry (Table 1 & 2) and support data for all the seismic zones. Apart from the preliminary (Gravity) loads, static earthquake analysis along with response spectrum analysis was carried out. The beam slab system and flat slab system modelled using SAP 2000 is as shown in Fig 1and Fig 2.

Table.1. Specifications of the buildings

Parameters	Beam slab system	Flat slab system
Grade of concrete	M 30N/mm^2	
Grade of steel	Fe 500 and Fe 415 N/mm^2	
Number of stories	G+5	
Beam size	300x600mm	
Beam cover	50mm	
Column size	300x600mm	
Column cover	40mm	
Slabs	150mm	In. Panels-150mm
		Drops- 250mm
Live load and finishes	3 kN/m^2 and 3kN/m^2	

Table.2. Seismic definitions

Zones considered	I, II, III and IV
Damping Ratio	5%
Importance factor	1
Type of Soil	II (Medium Soil)
Response Reduction Factor	5
Time Period	0.075xh$^{0.75}$

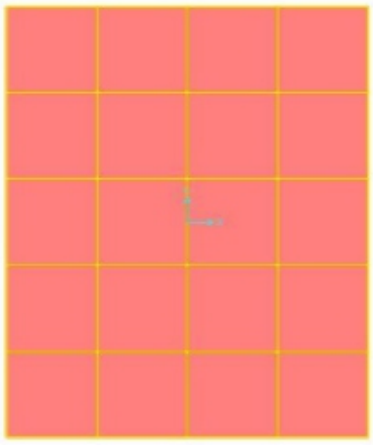

Fig.1. Beam slab model

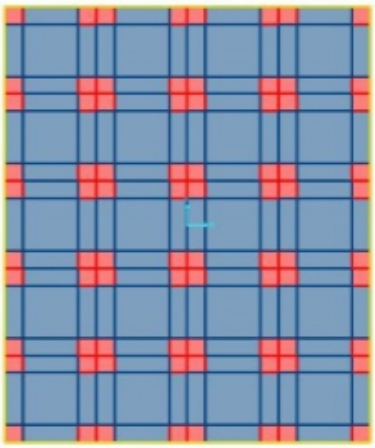

Fig.2. Flat slab model

2. PUSHOVER ANALYSIS

Pushover analysis was performed by subjecting lateral loads monotonically over the entire structure once after the gravity loads were assigned. The stiffness thus obtained from the gravity loads was considered as the initial load for lateral loads. Auto hinges of M3 for beams(Bending members) and PM2M3 for columns (Axial members) were assigned on either ends of the members along with P-Delta effect. Demand spectrum was developed by using response spectrum method and is super-imposed over the Displacement vs Base shear graph generated by the pushover analysis to get the performance point (Fig.4).Displacement controlled type of pushover analysis was performed. In this paper, pushover analysis was considered as a vital tool since it gives more précised seismic behaviour of the structure.

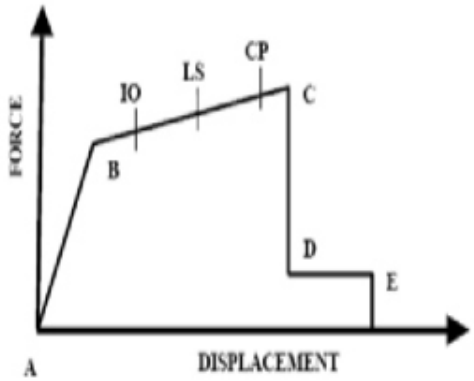

Fig.3 Force-Deformation curve

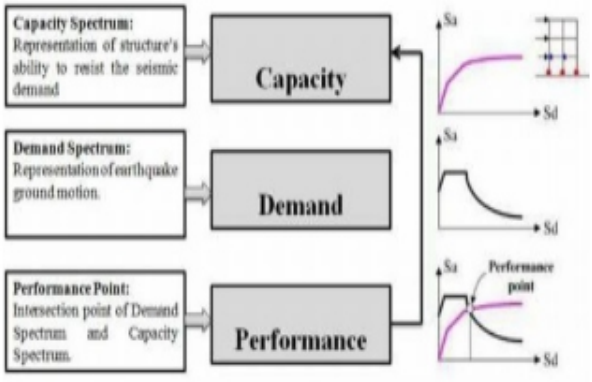

Fig.4 Spectrum Curve

(Source: http://www.engineeringcivil.com/evaluation-of-response-reduction-factor-for-rc-elevated-water-tanks.html)

Where,
A to B – Elastic state,
B to IO- below immediate occupancy,
IO to LS – between immediate occupancy and life safety,
LS to CP- between life safety to collapse prevention,
CP to C – between collapse prevention and ultimate capacity,
C to D- between C and residual strength,
D to E- between D and collapse
>E – collapse

3. RELIABILITY ANALYSIS

Uncertainties like Geometric-breadth, depth and cover of beams and columns, Materialistic- fck , and as well as loads on the slabs are calculated by Monte Carlo simulation technique using Excelconsidering the standard deviation values(Table 3). Random pushover analysis was carried out by considering all these values to get the randomized results of performance point, safety index and as well as differential hinge patterns.Basically Monte Carlo Simulation was used to carry out risk analysis by giving predefined probability distribution of an uncertainty. In this technique random values were obtained from the probability distribution for any number of values that are needed.

Table.3. Reliability analysis definitions (Source: Ranganathan&Ellingwood)

Specifications	Standard deviation
	Breadth- 9.47
	Depth- 9.38
Beams	Cover- 8.41
	Breadth- 5.69
	Depth- 7.89
Columns	Cover- 12.13
fck	3.04
Loads	1.6

Results and discussions

The following are the Displacement vs Base shear graphs for both beam slab and flat slab system for all the seismic zones.

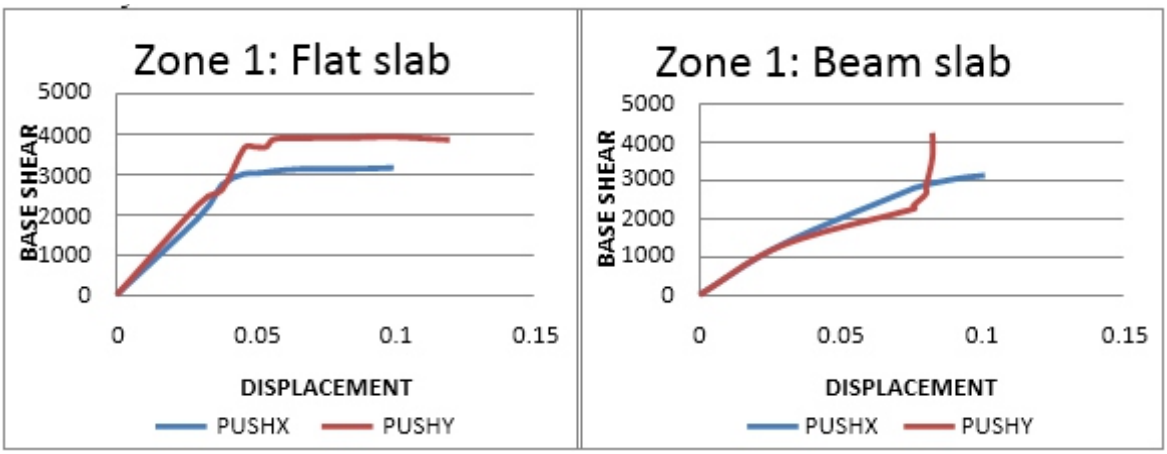

Fig.5 Pushover curve Z1 FS **Fig.6 Pushover curve Z1 BS**

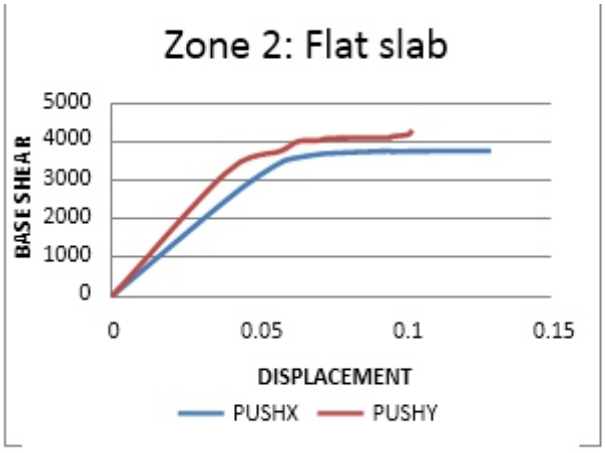

Fig.7 Pushover curve Z2 FS

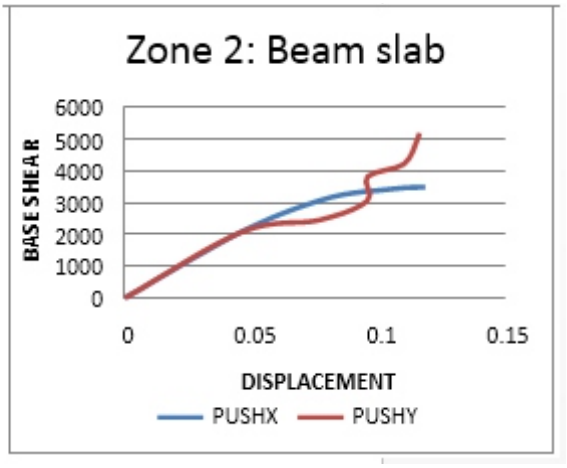

Fig.8 Pushover curve Z2 BS

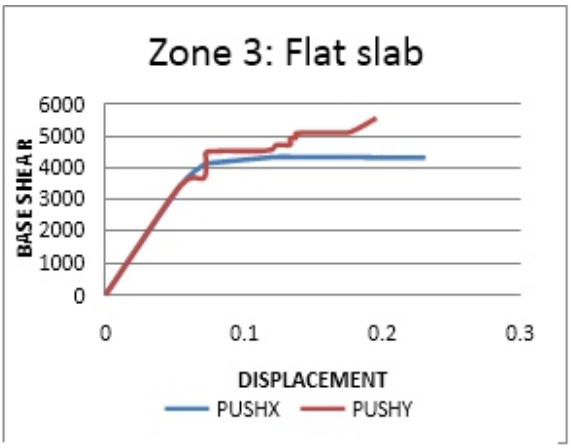

Fig.9 Pushover curve Z3 FS

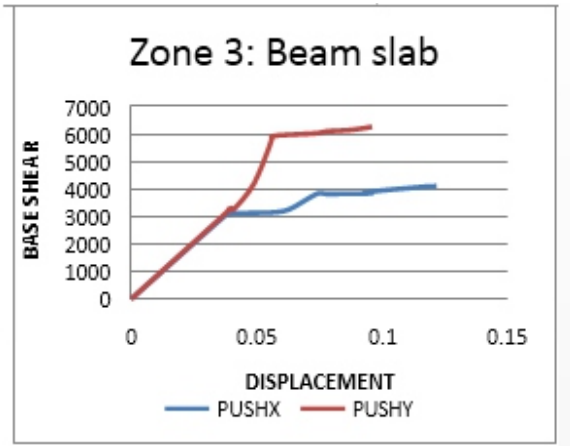

Fig.10 Pushover curve Z3 BS

Fig.11 Pushover curve Z4 FS

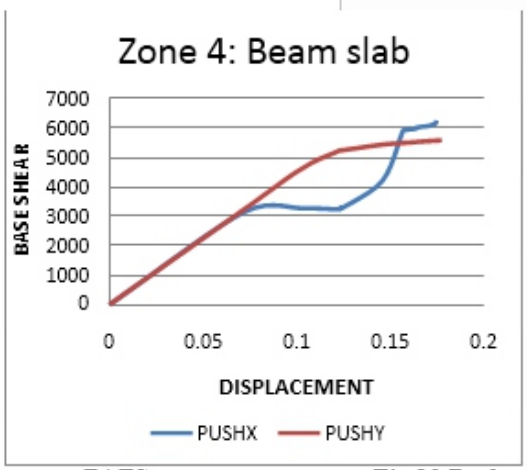

Fig.12 Pushover curve Z4 BS

From the above graphs we can see that the base shear value increased as the seismic zone value increased, and also that the base shear value for flat slab is higher than that of the beam slab structure.

Table.4. Plastic hinge formations

SYSTEM	ZONES	CASE	A-B	B-IO	IO-LS	LS-CP	CP-C	C-D	D-E	>E	TOTAL
BS	Z1	PX	680	250	18	0	0	0	0	0	948
		PY	780	168	0	0	0	0	0	0	948
FS	Z1	PX	306	270	0	0	0	0	0	0	576
		PY	401	175	0	0	0	0	0	0	576
BS	Z2	PX	656	270	22	0	0	0	0	0	948
		PY	760	188	0	0	0	0	0	0	948
FS	Z2	PX	251	303	26	0	0	0	0	0	576
		PY	356	220	0	0	0	0	0	0	576
BS	Z3	PX	580	326	40	2	0	0	0	0	948
		PY	572	376	0	0	0	0	0	0	948
FS	Z3	PX	238	296	38	4	0	0	0	0	576
		PY	332	244	0	0	0	0	0	0	576
		PX	600	269	70	9	0	0	0	0	948
BS	Z4	PY	646	302	0	0	0	0	0	0	948
FS	Z4	PX	309	166	88	13	0	0	0	0	576
		PY	295	281	0	0	0	0	0	0	576

Table.5. Performance point

Zone	System	Load case	Performance point (kN)	Displacement (m)
Zone 1	Beam slab	PUSHX	1352.32	0.027
		PUSHY	1737.1	0.002114
	Flat slab	PUSHX	2920.57	0.03
		PUSHY	3894.88	0.00246
Zone 2	Beam slab	PUSHX	2145.9	0.047
		PUSHY	2672.47	0.00233
	Flat slab	PUSHX	2890.8	0.048
		PUSHY	3873.9	0.00335
Zone 3	Beam slab	PUSHX	3190.2	0.067
		PUSHY	3921.51	0.00273
	Flat slab	PUSHX	3956.63	0.072
		PUSHY	4310.83	0.00464
Zone 4	Beam slab	PUSHX	4766.68	0.101
		PUSHY	5769.46	0.00385
	Flat slab	PUSHX	6094.45	0.107
		PUSHY	6328.6	0.00618

CONCLUSIONS

- Results shows that the plastic hinge formations are more in flat slab system when compared to beam slab system.
- Flat slab system has higher values of performance point and target displacement than that of Beam slab system.
- Beam slab building has 8% increase in the hinge formations when reliability analysis is carried out and whereas Flat slab building shows 19% of increase.
- Beam slab building has safety index of 5.41 and Flat slab has 4.95 with respect to base shear values.

REFERENCES

[1] HardikBhendadia " Pushover analysis of RC frame structure with floating column and soft story in different earthquake zones" IJRET, Volume 4 Issue 4, 2015

[2] Prof. Milind" Pushover analysis of structures with plan irregularity" IOSR journals, Volume 12 Issue 4, 2015

[3] KallolBarua"Performance based analysis of seismic capacity of mid rise building" IJETAE, Volume 3 Issue 11, 2013

[4] Da-Gang Lu "global seismic reliability analysis of building structures based on system- level limit states" 14 WCEE, 2008

[5] T.D. GunneswraRao "Probabilistic Assessment on Flexural Strength of Steel Fiber Reinforced Concrete Members" IJERGS, Volume 3 Issue 1, 2015

[6] Sukanti Rout "Monte Carlo Simulation Technique For Reliability Assessment Of R.C.C. Columns, IJERA, Volume 2 Issue 5, 2012

Diagnosing the Faulty Model of A Motor Based on Fft Analyzer with Vibrating Analysis

Bharathi S L*, N. Pritha*, N. Arunpriya*, R.Preethi ** ,A. Murali***

*Department of Electronics & Communication Engineering, Panimalar Engineering College, Chennai, India

** Department of Information Technology, Panimalar Engineering College, Chennai, India.

*** Department of Electronics & Communication Engineering, Miracle Educational Society Group of Institutions, Bhogapuram, Visakhapatnam, A.P, India

ABSTRACT

The most of the signal analysis techniques which rely on spectral approaches plays a vital role in the diagnosing a variety of vibration related problems in the rotating machines. One of such techniques is known to be as the Fast Fourier Transform (FFT). In the critical machines, there is a continuous online monitoring system. This ability provides the early detection of the faults and protective action is established with high reliability. In this paper, we described the fault and un-fault models of the machine, with chosen hardware and software solutions. By integrating the traditional algorithm with rule-based for fault detection, has the advantageous approach, especially the fault diagnostic high performance of the machinery, which is more than 99% correctness in all of the situations.

Keywords: Spectral approach, Rotating machines, Fault model, Un-fault models Fault diagnostics

1. INTRODUCTION

In the field of signal analysis techniques, based on the fast Fourier transform, diagnosing of on-line and rotating machinery are very effective in analyzing the vibration [1]-[5]. The analysis of the vibrating signals is obtained with the two domains namely time-domain and frequency-domain. As mentioned in [6]-[8], the time domain approach, it is not successful in the multi-tone vibration signals as a complete insight is provided. But the frequency domain approach allows identifying the phase spectrum and the amplitude. [9] and [10] noticed that, the resulting spectrum must be diagnosis to obtain the more valid information after the further processing of the vibrating signal.

The instrument that is commonly used in the vibrating analysis only in the frequency domain in Dynamic Signal Analyzer (DSA) [11]. It enables to evaluate the changes in the spectrum in time, and time-limited event. The other DSAs which are also used for the vibration analysis, based on the elaborating speed, display resolutions, cost and portability of the system. Some of them are handheld, benchtop instruments, computer-controlled systems are on the market. The primary goal of the continuous on-line monitoring system is that early alarm and the correctness in the data acquisition. The following are some of the requirements for an effective vibration analysis for the on-line monitoring system.

1. Real-time analysis
2. Optimum choice of measurement values (sampling frequency, number of points, window function) for sensitivity in the fault identification [12].
3. Integrated software diagnostic system in DSA for determining the fault severity.

But unfortunately, these requirements cannot be satisfied by the general-purpose instruments. In fact,

1. Visualization of the spectrum is more time consuming. In real-time, the spectrum evaluation cannot be performed in most of the DSAs.
2. As there is no automatic configuration phase, the DSA set-up is not that efficient.
3. There is no availability of exchange of data in the DSA and diagnostic software in the real-time scenarios for on-line fault isolation.

In the real-time practices, the authors designed an intelligent FFT analyzer for high performance states[13]&[14]. The configuration procedural development evolves an automatic adaption of the operating parameters in signal spectrum. This instrumentation is customized in typical applications like tone monitoring, detection etc. For as in the real-time practices, the usage of 50- kHz band-with signals are needed in the two-DSP parallel architecture for analysis processes. We also described for a brief understanding the customized intelligent FFT analyzer for modifying the software [15]. The model-based diagnostic approach [16], [17], consists of pattern matching procedure that detects and isolates the fault by comparing the actual device with both fault and un-fault models.

This experiment primarily shows the identification of fault and un-fault models, secondly the designed measurement system with hardware and software characteristic features. Lastly, the proposed technique is then verified with various faulty and un-faulty operating conditions for witnessing the high performance of the system.

2. RECOGNIZING THE FAULTY AND UN-FAULTY MODELS

In the model based diagnostic approach, the identification of the faulty and un-faulty model identification is required. This consists of suitable parameters of vibration signal spectra in the frequency-domain analysis. Some of the studies as mentioned earlier presents the relations among the defects and the characteristics of the vibrations in the electrical machinery systems.

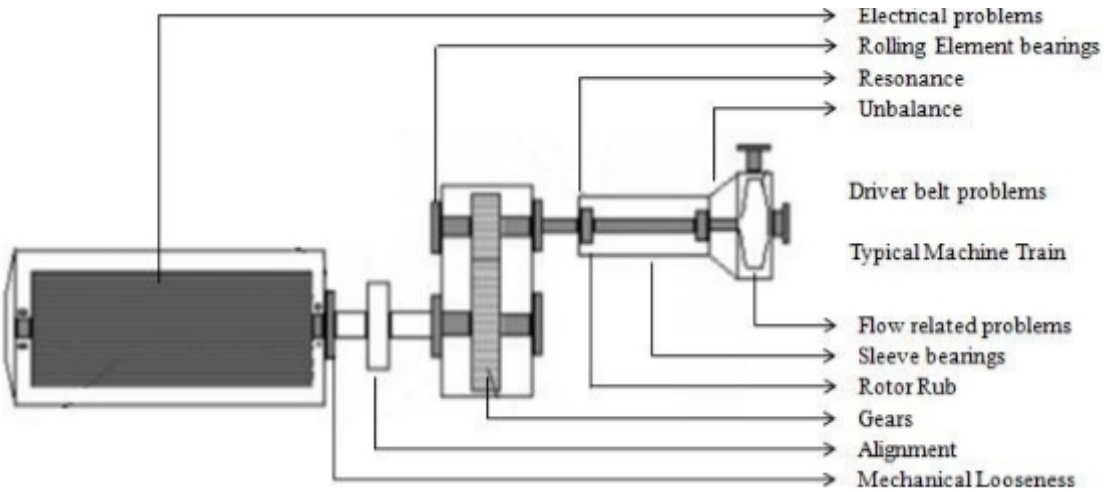

Figure 1: Electrical Machinery fault detection

When detecting the un-faulty operation of the vibratin spectrum, tones located in the shaft rotating frequency, the number of harmonics with amplitude is less than one-third of the amplitude of rotating frequency are generated. The following figure 2 shows the example of waveforms comparing in the wave terminology.

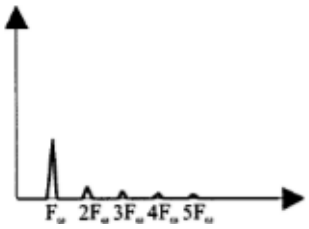

Figure 2: Figure 1: (a) Un-Faulty Model

In the presence of gear, there exists three main additional tones appeared as - one at the running speed of the low-speed shaft, one at running speed of high-speed shaft and one at the gear mesh frequency. Where the Fw is the shaft rotating frequency. The other tones are generally goes under the un-faulty signal spectrum due to the vibrations of the structure as the motor is plugged on. Every kind of the machinery system failures needs specific alteration among the spectrum vibration analysis with respect to the un-faulty models. The figure 2 shows graphical notations for some common faults that occur in the systems. These characteristics defines the numerical and the logical model parameters. The number of tones, the fundamental(Fw), amplitude of first five harmonics of Fw, amplitude ratios between second harmonic(2Fw) and the sum of all tone amplitudes are comes under numerical parameters. The frequencies like Out Ball Pass Frequency, Inner Ball Pass Frequency comes under the category of logical parameters.

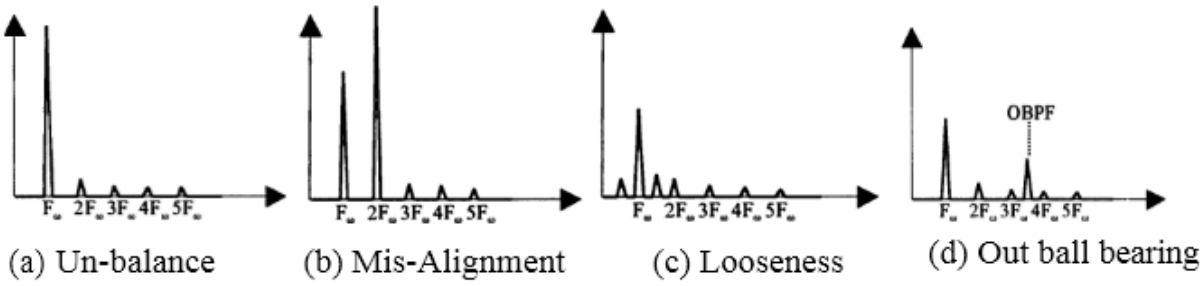

Figure 2: Faulty Models

The following figure 3 gives the resultant values of the un-faulty and faulty models on the real-time data. This point out the clear differences between the vibrating spectra.

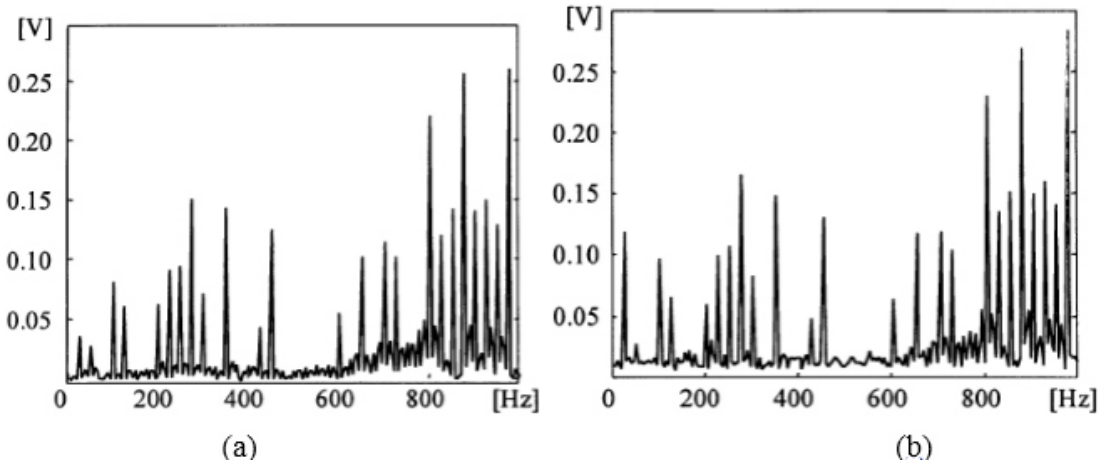

Figure 3: (a) Un-Faulty Spectrum ; (b) Modified frequency with 25Hz

It is impossible to generate a desired time instants when the motor in under operational mode. Since the in the real-time scenarios, the diagnostic systems cannot be reversible to recognize the faults in the machinery systems. To overcome this effective problem, a specified procedure is introduced based on the fault emulation. A suitable processing of un-fault signal performed by an arbitrary waveform generator. It has a special feature that allows the modification of the frequency in order to generate a fault spectrum as in figure 3. The use of an arbitrary waveform generator also allows the fault to be produced in any instant of the machine operation, by using test sequences composed of un-fault and fault subsequences. The correctness of the proposed emulated approach can then be verified by producing some reversible faults on the machine under test.

2. DESIGN SYSTEM OF A VIBRATION ANALYSIS

Some of the designed systems of a specific class motors are optimized in the hardware and the software applications. They are small-size, three-phase, two-pole pair, and asynchronous motors. This customization will not reduce the generality of the proposed design, as the hardware and the software are highly reconfigurable.

3.1 Hardware Design of the FFT Analyzer:

The Designed system of the vibration analysis for the fault diagnosis is typically works for the small-size electrical motors. From the figure 4, the system consists of

1. Acceleration sensor – 8710A50M1 characterized by:

Low output impedance (about 100), 6 kHz upper cut-off frequency, 1000 mV/g sensitivity, 5 g measuring range, and 51 g of mass loading.

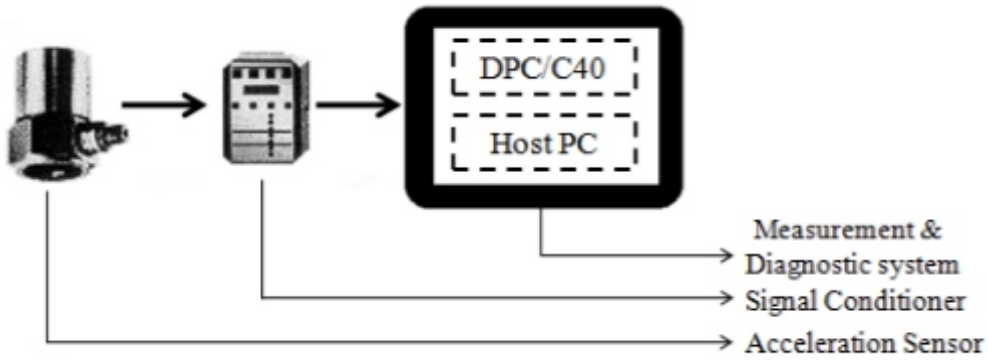

Figure 4: Block diagram of the Designed System

The accelerometer is magnetically mounted directly on the motor under monitoring, in order to assure an optimum coupling.

1. Signal Conditioner – 5118B1 is used to adapt the sensor output to the input range of the acquisition and the elaboration section.

2. Measurement and Diagnosis system – It is based on the PC-bus compatible carrier board and DPC/C40 with two concurrent DSPs and an on-board data acquisition system.

The two mounted DSPs are the TMS320C40 by Texas Instruments™; they use a floating-point numerical representation with 32 bits, and work at 40 mHz. The DSPs are in a Master/Slave configuration (only the Master DSP can directly access the board resources), and communicate by using

six serial ports. The ADM is featured by two Delta-Sigma ADCs and two DACs with 16-bit resolution, 200 kHz maximum sampling frequency, V full-scale, and 20 k input impedance. The data transfer between the Master DSP and the host PC is carried out by using a shared 4 K 32-bit memory.

3.1 Software Design system

The previous discussions on the measurement system are based on the monitoring and diagnostic capabilities which are only possible with the dedicated software analyzers. These are divided into three types corresponding to the three steps needed to achieve the on-line monitoring and diagnosis. These procedures are implemented on DSPs in order to optimize the response time.

The signal processing: This software uses two DSPs in parallel execution, analyzes the vibration signal in the frequency domain, and evaluates the characteristics of its spectrum, chosen for representing the actual model of the motor under test. The software for the on-line spectrum evaluation is an optimization of the intelligent FFT-Analyzer measurement procedure [9] and [10], on the basis of the knowledge of the un-faulty vibration spectrum and on the expected fault ones. The measured un-fault spectrum (see Figure. 5(a)) has tones up to 8 kHz, and consequently the sampling frequency has to be fixed at 16 kHz to avoid aliasing. Theoretical analysis reported in the literature applied to the motor under test suggests that the considered faults give rise to additional meaningful tones not higher than 1 kHz. Thus, to improve the frequency resolution, the acquired signal is filtered (30th order FIR filter with 1.1 kHz cut-off frequency) and decimated (decimation factor = 4).

A dedicated algorithm performs the two operations in a single step [10], allowing a meaningful reduction of the computational load. The so-obtained sample sequence (2048 points) is windowed, and the FFT is evaluated. To identify the signal tones, the amplitude spectrum must be analyzed [10]. Then the frequency and the amplitude for every tone is interpolated with the samples of FFT [18], [19]. Finally, the numerical and the logical parameters can able to be estimated in the actul model of a motor. Table I reports the maximum elaboration times of each step of the signal-processing procedure. These times do not allow a diagnostic activity to be carried out at each sampling, but they are perfect in timing usually expected for the monitoring of apparatus working at industrial frequencies.

The fault detection: After completion of each signal processing procedure, the comparison goes on with the referenced un-faulty vibrations for fault detections. The high variability in successive measurements with some motor operating conditions, suggests the use of a statistical approach for identifying the reference vibration spectrum model parameters. In particular, the vibration spectrum in the absence of faults was calculated 20 times. Figure 5(b) reports the mean values and the variability of each tone amplitude, estimated as three times the standard deviation. As for the frequency variations, they prove to be always contained within ±0.5Hz around the measured mean values. A weighted squared sum of the difference between actual and un-fault numerical parameters is continuously evaluated and compared with a suitable threshold. In order to avoid false alarms, a fault is highlighted only when the threshold is overcome, or a check is positive in two subsequent spectrum analyzes.

The fault diagnosis: A correct fault diagnosis requires reasoning on spectrum parameters referring to a complete fault time interval. Consequently, the fault isolation procedure is activated on the signal processing results obtained after the fault detection. A rule-based diagnostic procedure was directly implemented on the Master DSP rather than on the PC, in order to obtain better time performance. First the checks on the logical parameters are performed, allowing the related faults to be highlighted or discarded.

For an example, a defect in the outer race of the ball bearing gives rise to a tone at OBPF. In these cases, the diagnostic procedure stops, and only the corresponding fault is given with a certainty factor equal to one. Table II reports the kind of faults that are identified by these demons with the corresponding characteristic frequency. If no one of these conditions is verified, the procedure goes on applying rules focused on increasing the certainty factor of other possible faults.

In particular, for each fault, the certainty factor is increased as a function of the distances between the actual model and its fault model. The certainty factors were tuned in the set-up phase in order to optimize the diagnostic performance.

Table I: Maximum Elaboration time for two different algorithms of signal processing procedures

Algorithm	Filtering + Decimation	Windowing + FFT	Tone detection + interpolation + model parameter estimation
Elaboration Time	70 ms	11 ms	3 ms

Table II: Fault detection by Demons, frequencies and the causes of occurrences

Fault detection	Frequency (Hz)	Occurance
Looseness	12.5 - 37.5	0.5-1.5 F_ω
OBPF	127.5	Out ball bearing dimension
IBPF	112.5	Inner ball bearing dimension

The output of this procedure is a list of probable faults, each with its certainty factor. A fault is considered as ―probable‖ if its certainty factor is greater than a suitable threshold (0.5) [20], [21].

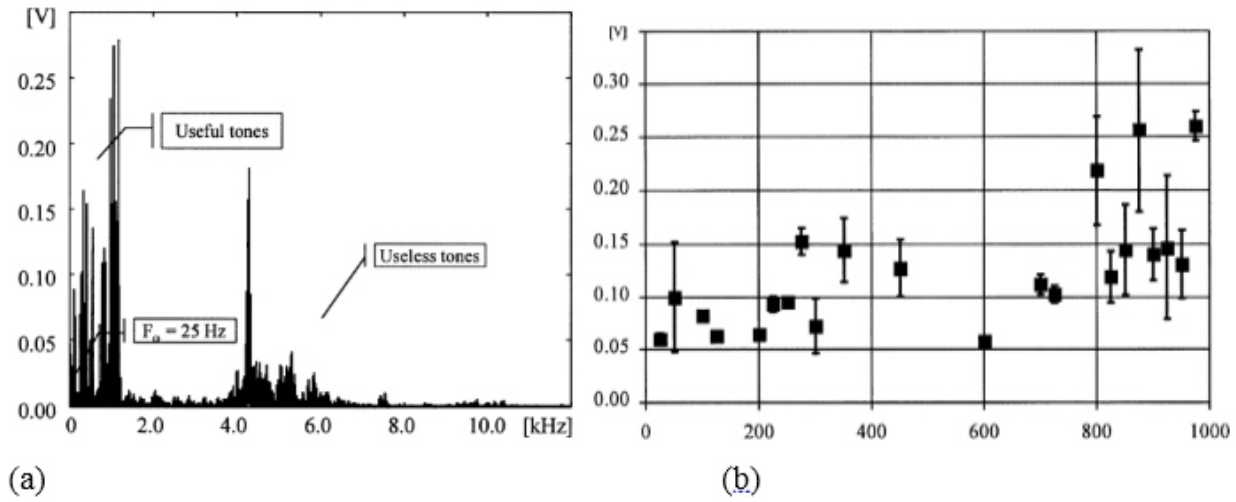

Figure 5: (a)Un-fault vibration spectrum ;(b)Un-faulty conditional values with measured tones This diagnostic list is also passed by the Master DSP to the PC via Shared Memory. The DSP Master executes this fault diagnosis procedure, taking about 0.02 ms.

4. EVALUATING THE SYSTEM DIAGNOSTIC PERFORMANCE

As for the performance evaluation, in terms of diagnostic capabilities and response time, of the designed instrument, numerous experimental tests using real and emulated signals are carried out. The false alarm rate is evaluated by running the diagnostic procedure during the motor normal operation in different working conditions. No false alarm occurs in 20 tests lasting 30 min each. More than a hundred tests for each fault were carried out, and the obtained diagnostic results in detailed. The performances of the fault detection procedure are expressed in terms of correct and missed detection percentages. For the diagnostic procedure, some classes are identified, and the percentages of each class are reported in the Table III.

Table III: Diagnostic performance of the Designed System

Fault Type	Correct Location	InCorrect Location	Missed Location	Quasicorrect Location	Correct Detection	Missed Detection
Unbalance	99.5	0	0	0.5	99.5	0.5
Mis-Alignment	99	0	1	0	99.5	0.5
Looseness	99	0	1	0	98.5	1.5
Outer ball bearing	99.5	0	0.5	99.5	100	0

The arbitrary signal generator can provide an additional signal (marker), with only two amplitude levels (0–2 V), that can be synchronized with the generation of a specific sample. The fault instant can be exactly identified by synchronizing the marker with the beginning of the fault signal in the sequence. On the other hand, one ADM D/A converter can be used for highlighting the instants in which the DSP-based system reaches the detection and the diagnosis. In particular, a 3-V voltage pulse is generated as soon as a fault is detected and when the diagnostic process is ended. These two signals are displayed on a digital oscilloscope (Tektronix TDS 520D, 500 MHz bandwidth, four input single-ended channels), allowing the response time of both fault detection and fault diagnosis to be measured (see Fig. 6).

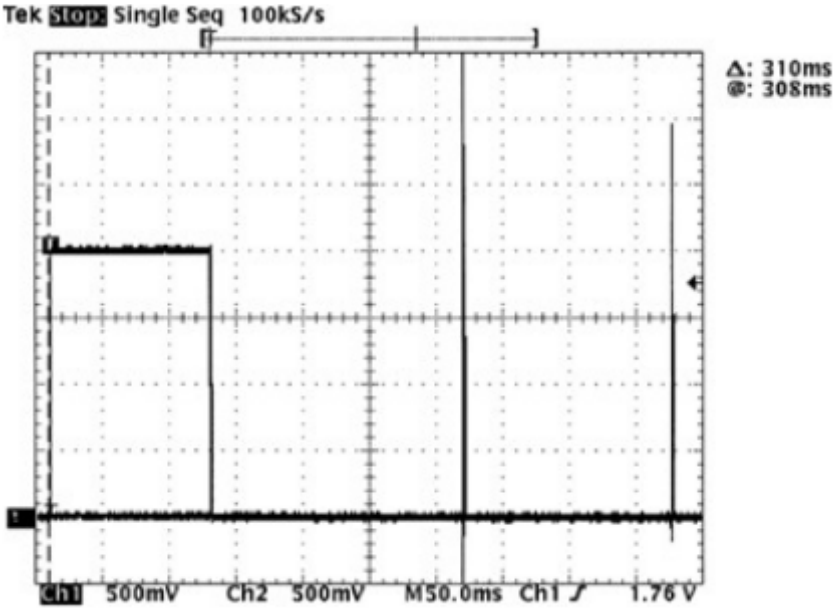

Figure 6: An example of a response time

The measured response times are not constant since they depend on a number of factors; a mean delay of 300 ms for the fault detection and of 470 ms for the diagnosis is measured. A set of unbalance faults was also produced on the motor in order to check the proposed fault model as well as the emulated approach.

Different values of the weights (77.5 g, 65 g, and a couple of 40 g weights) are placed on the shaft at different angles, in order to test the system for different faults of this class. Diagnostic results in optimum agreement with the one obtained by the emulation approach were obtained.

5. CONCLUSION

In this paper, we described a DSP-based architecture for vibration analysis. It allows machine to on-line monitoring, with a consequent increase in the system and in environmental safety. The integration of the traditional signal-processing algorithm with rule-based reasoning for fault detection and isolation presents many advantages, especially concerning the diagnostic performance of the system, with correct diagnosis in more than 99% of the situations. The emulation-based method used to estimate the vibration signal in the faulty condition proves to be very effective and can be easily extended to numerous application fields.

REFERENCES

[1] W. R. Finley, M. M. Hodowanec, and W. G. Holter, —An analytical approach to solving motor vibration problems,‖ IEEE Trans. Ind. Applicat., vol. 36, pp. 1467–1480, Oct. 2000.

[2] A. Ypma and P. Pajaunen, —Rotating machine vibration analysis with second-order independent component analysis,‖ Proce. IEEE Int. Workshop Independent Component Analysis Signal Separation, 1999.

[3] S. Nandi and H. A. Toliyat, —Condition monitoring and fault diagnosis of electrical machines—A review,‖ in Record 1999 IEEE Thirty-Fourth IAS Annu. Meeting Conf. Industry Applicat. Conf. , vol. 1, 1999, pp. 197–202.

[4] J. S. Mitchell, Introduction to Machinery Analysis and Monitoring, 2nd ed. Tulsa, OK: Pennwell, 1993.

[5] C. M. Riley, B. K. Lin, T. G. Habetler, and R. R. Schoen, —A method for sensorless on- line vibration monitoring of induction machines,‖ IEEE Trans. Ind. Applicat., vol. 34, pp. 1240– 1245, Dec. 1998.

[6] S. L. Marple, Digital Spectral Analysis, with Applications. Englewood Cliffs, NJ: Prentice-Hall, 1987.

[7] M. Kay and S. L. Marple, —Spectrum analysis—A modern prospective,‖ Proc. Inst. Elect. Eng., vol. 69, 1981.

[8] S. Jangi and Y. Jain, —Embedding spectral analysis in equipment,‖ IEEE Spectrum, pp. 40–43, 1991.

[9] B. Li, M. Y. Chow, Y. Tipsuwan, and J. C. Hung, —Neural-network-based motor rolling bearing fault diagnosis,‖ IEEE Trans. Ind. Electron., vol. 47, pp. 1060–1069, Oct. 2000.

[10] A. Dimarogonas, Vibration for Engineers. Englewood Cliffs, NJ: Prentice-Hall, 1996.

[11] —Effective Machinery Measurement Using Dynamic Signal Analyzers,‖ Hewlett Packard, Applicat. Note 243-1, 1990.

[12] C. Offelli and D. Petri, —The influence of windowing on the accuracy of multifrequency signal parameter estimation,‖ IEEE Trans. Instrum. Meas., vol. 41, pp. 256–264, Apr. 1992.

[13] G. Betta, C. Liguori, and A. Pietrosanto, A multi-application FFT-analyzer based on a DSP architecture, in IEEE Trans. Instrum. Meas., pp. 825–832, 2001, to be published.

[14] G. Betta, M. D'Apuzzo, C. Liguori, and A. Pietrosanto, —An intelligent FFT-analyzer,‖ IEEE Trans. Instrum. Meas., vol. 47, pp. 1173–1179, Oct. 1998.

[15] A. Bernieri, G. Betta, and C. Liguori, —Setting up and characterization of multiple-DSP measurement stations,‖ in Proc. IMEKO TC-4 Int. Symp., Budapest, Hungary, 1996, pp. 282– 285.

[16] R. J. Patton, J. Chen, and S. B. Nielsen, —Model-based methods for fault diagnosis: Some guidelines,‖ Trans. Meas. Control, vol. 17, pp. 73–83, 1995.

[17] A. Baccigalupi, A. Bernieri, and A. Pietrosanto, —A digital-signal-processor-based measurement system for on-line fault detection,‖ IEEE Trans. Instrum. Meas., vol. 46, pp. 731– 736, June 1997.

[18] C. Offelli and D. Petri, —Interpolation techniques for real-time multifrequency waveform analysis,‖ IEEE Trans. Instrum. Meas., vol. 39, pp. 106–111, Feb. 1990.

[19] G. Andria, M. Savino, and A. Trotta, —Windows and interpolation algorithms to improve electrical measurement accuracy,‖ IEEE Trans. Instrum. Meas., vol. 88, pp. 856–863, Aug. 1989.

[20] G. Betta, M. Dell'Isola, C. Liguori, and A. Pietrosanto, —Expert systems and neural networks for instrument fault detection and isolation,‖ in IEEE Workshop "Emerging Technol. Virtual Syst. Instrum. Meas.", Niagara Falls, ON, Canada, 1997, pp. 39–48.

[21] G. Betta, M. D'Apuzzo, and A. Pietrosanto, —A knowledge-based approach to instrument fault detection and isolation,‖ IEEE Trans. Instrum. Meas., vol. 44, pp. 1009–1016, Dec., 1995.

Modeling and Control of Fuel Cell Power Plant Using PID Controller

Satish Kumar*, Govind Kumar Maurya**

* M. Tech Student, School of EEE, Ajay Kumar Garg Engineering College Ghaziabad, U.P., India

** Assistant Scientific Officer, National Institute of Plant Health Management, Rajendranagar, Hyderabad, TN. India

ABSTRACT

In this paper going to represent about fuel cell. Fuel cells model going to use PEMFC 6kW- 45V Vdc to boost the voltage up to 48%. This is proton exchange polymer electrode membrane fuel cell. Fuel cells are going to controlled and boost the voltage supply using DC-DC voltage converter or chopper. In this paper going to improve the efficiency of the fuel cell is 55.56%. Fuel cell is the upcoming very good resource of the energy. It has a high efficiency and reliability, due to chemical reaction low pollution. A control strategy for these system using PID controllers is simulate here, with the help of Simulink. The significance of heating section in the overall performance is also analyzed. A smart energy arrangement and get a reinforcement control arrangement as a side advantage. Using MATLAB/SIMULINK analysis of efficiency and boost output power.

Key Words: Fuel-Cell Power Plant, SOFC, DC-DC Converter, PID Controller, Smart Energy

INTRODUCTION

"Earth has enough resources to meet people's needs, but will never have enough to satisfy people's greed" and “The people on earth should act as 'trustees' and use natural resources wisely, as our moral responsibility to ensure that we bequeath to the future generations a healthy planet.”- Mahatma Gandhi [1].

In now day requirement of fossil fuels is most important part in daily life. As per the increasing the passage of time. More consumption of fossil fuels will raises the greenhouse gas emissions in the environment and cause the grat pollution i.e. become the global problem. This greenhouse gas will only reduce when reducing consumption of fossil fuels and the people to use the renewable energy sources [1]. In that area of technology production of hydrogen from the renewable the sources of the energy are procedure of development and showing. In order to meet the requirement of future energy demands and eco-friendly manner, technology to developed the production for the storage and application of hydrogen transportation and generation of electricity [13]. As per daily the populations and industries are increasing day by day the emission of CO2, nitrogen, sulfur oxide and other polluted gas increases. According to data of United Nations, the word population will reach 8 billion in spring of 2024 and 9 billion by 2050 [1]. According to government data the emission of CO2 will not rise more than 450 ppm by the 2050 in the word level signed among the countries, but in 2009 it was 415ppm and will be 430ppm by 2025.

Fuel cell is defined an electrochemical cell which unlike to storage cells. Fuel cell is continuously contact with the fuel and electrical power output independently [3]. It changes over hydrogen or hydrogen containing powers, straightforwardly into electrical vitality in addition to warm through the electrochemical response of hydrogen and oxygen into water. In expansion to the energy unit stack, a

power device control plant incorporates a fuel processor and subsystems to oversee air, water, and warm vitality, and power. The fuel is provided under certain weight to the anode side of the energy component [4-5].

$$H_2 \rightarrow 2H^+ + 2e^-$$

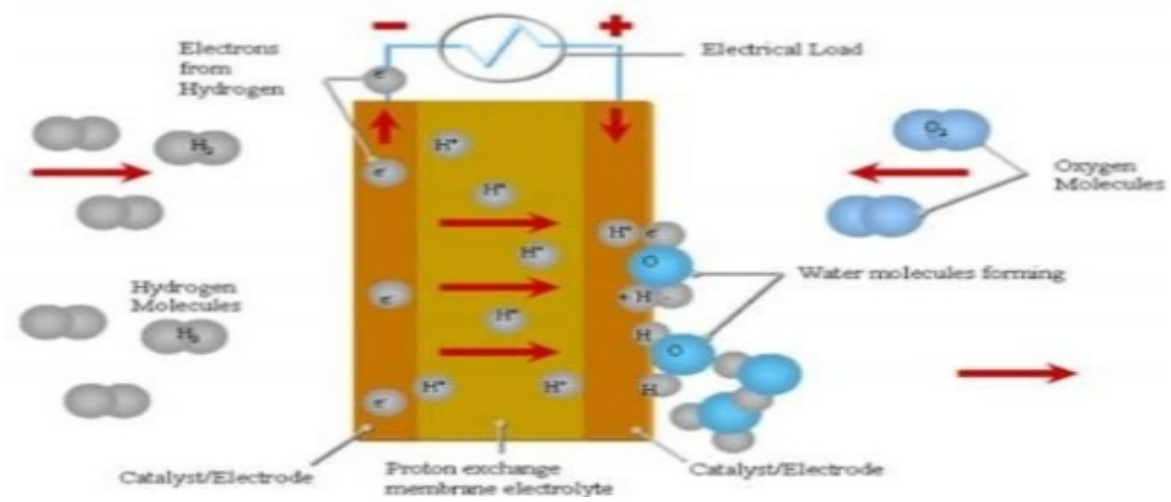

Figure 1: Working of fuel cell [7]

The protons are exchanged through the electrolyte (strong film) to the reactant layer of the cathode. On the other side of the cell, the oxidizer moves through the channels of the stream field plate and responds on the synergist layer of the cathode. The oxidizer utilized as a part of this model is air or O2. The oxygen consolidates with the protons and electrons to shape water, alongside arrival of little measure of warmth, on the surface of the reactant particles.

$$2H^+ + 2e^- + 1/2O_2 \rightarrow 2H_2O$$

Energy component control plant innovation is being developed, world over and outline, acknowledgment and operation techniques are being created. The paper portrays one of the conceivable approaches in actualizing control procedure for a PEM Fuel cell control plant. The idea was actualized on a test display PEM control plant effectively and extremely helpful sources of info have been determined.

I. PEM AND SOEC FUEL CELL OPERATION

Biomass gasifier-SOFC based power plants. Two unique SOFC framework setups were considered. The two coordinated frameworks have the same biosyngas generation framework utilizing a downdraft settled bed gasifier and a gas refinement framework utilizing both high and low temperature gas cleaning advancements. The contrast between these two frameworks is the SOFC framework setup. The SOFC framework has an ejector-driven anode distribution, no distribution is utilized in the energy unit framework, and however an immediate fuel conveyance framework that supplies the biosyngas to the SOFC stack is utilized. Execution of these two frameworks was assessed regarding vitality and energy efficiencies.

The PEMFC has a many advantage in compare of other fuel cells [3].

- PEM has highest power density 300-100nW/cm^2
- Easily start stop capability
- Very low temp operation for portable application

- More reliable than other fuel system
- They have very less moving part
- Easily refueling
- It is a higher energy density in compare to batteries in term of potential

III. FUEL CELL POWER PLANT

A fuel cell power plant consist of a fuel cell stack, a fuel supply system, devices like inlet and outlet solenoid valves, humidifier water heater, humidifier water pump, coolant pump, gas heaters, mass flow controllers, recirculation blowers, humidifiers and a control system. Here is the simple block diagram are shown in figure 2. In this only fuel cell stack, DC-DC converter and PID controller and other are inbuilt in the fuel cell stack.

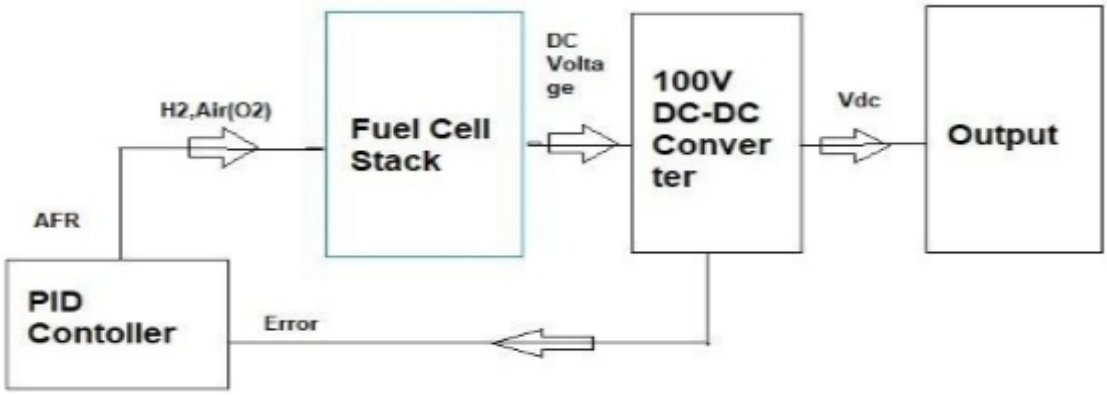

Figure 2: Basic Block Diagram of Fuel Cell with DC-DC Converter

A. Fuel Cell Stack:

The subsystems engaged with the energy unit control plant incorporates predominantly the accompanying: Electrode Stack, Gas Administration System, Water Management System, Gas Warming System, Thermal Management System, Operation furthermore, Control conspire.

The water heating consist of electrically power heater. The water inlet and maintain the suitable level. Then water outlet into the humidity section. Fuel cell load power deliver to the load.

P = E • I

Power = Voltage • Current

$$watt = \frac{joule}{s} = volt \cdot \frac{coulomb}{s}$$

Intel reactant gasses are to be humidified before going into the power module stack. This is too fundamental to guarantee the conductivity of the film electrolyte in the cell. Humidification of stack channel gasses is mandatory with a specific end goal to draw current from energy unit stack. The humidification of fuel and oxidizer fills two needs; rising of temperature of the gas and humidification from 0%RH to 100%RH.

$$\text{Gibbs free energy given by} \qquad E = -\frac{\Delta G}{nF}$$

Here n is the moles of electrons released for every mole of hydrogen reacted (2 mol e-/ 1 mol H2). Maximum voltage E.

The sub system of fuel cell stack that increase the humidity gas temp by 2-3°C, furthermore, cut down the relative moistness of gasses keeping in mind the end goal to maintain a strategic distance from buildup due to warm misfortune in the gas tubing line from humidifier to stack [6]. The buildup in the gas line may cause water flooding and discourage the gas stream in bipolar plate channels.

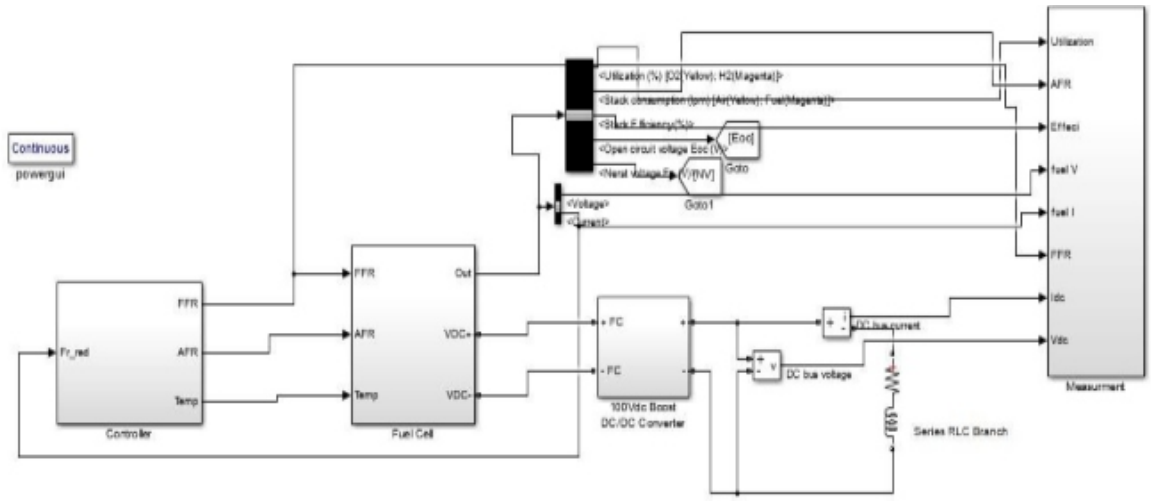

Figure 3: Power Fuel Cell Matlab/Simulink Model

B. DC-DC Converter

The output of the DC-DC controller is used to control the gate pulse of the switch in converter so that the output will match the reference value of voltage. Output of the converter is connected to the load the boost converter is higher efficient to the other DC-DC converter. In this paper the DC-DC converter 100V converter that produced a power up to 6kW. As shown in figure 4.

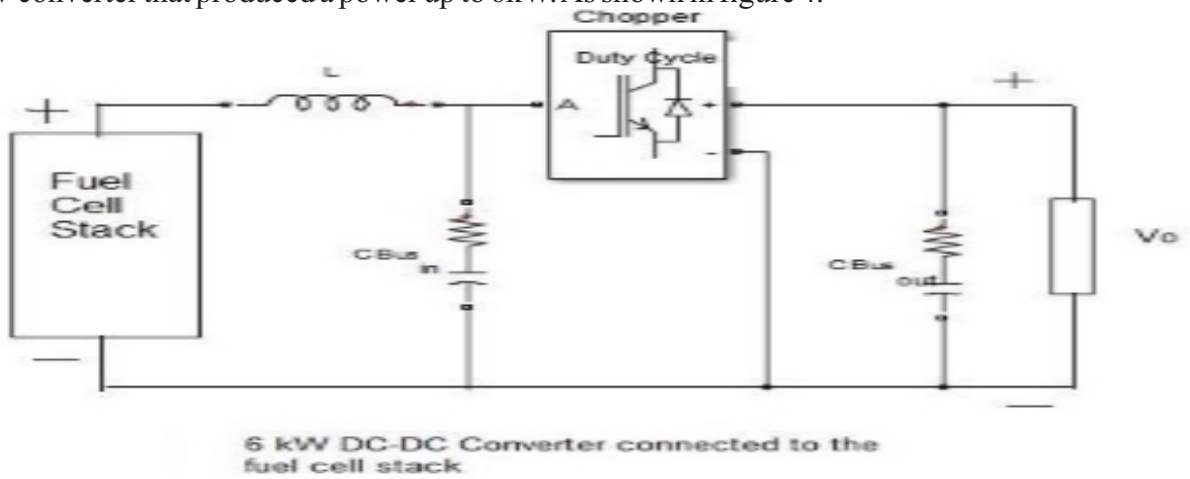

Figure 4: 6kW DC/DC converter connected with Fuel Cell Stack

$$\begin{bmatrix} \frac{di_L}{dt} \\ \frac{dv_{dc}}{dt} \end{bmatrix} = \begin{bmatrix} \frac{-R_L}{L} & \frac{(1-d)}{L} \\ \frac{(1-d)}{C} & 0 \end{bmatrix} \begin{bmatrix} i_L \\ v_{dc} \end{bmatrix} + \begin{bmatrix} \frac{d}{L} & 0 \\ 0 & \frac{1}{C} \end{bmatrix} \begin{bmatrix} v_{fc} \\ i_{ac} \end{bmatrix}$$

where Vfc and Vdc respectively stand for the voltage of energy unit and DC Bus, iL and iac speak to the current of inductor and yield current of inverter, L is the inductor with equal arrangement resistance RL, and C is the capacitance. At the point when the turn is on or off, the topology will venture down or up the yield voltage.

Today the larger part of high power PCSs are acknowledged with the DC/DC idea. Since the DC voltage created by a energy unit stack shifts generally and is low in size (<50 V for a 5 to 10 kW framework, <350 V for a 300 kW framework), a voltage balancing out stride up DC/DC converter is fundamental to produce managed higher DC voltage (600 V ordinary for 3×400 Air conditioning yield). A DC/AC inverter is basic for change of the DC to valuable AC control at 50 Hz recurrence. A yield LC channel associated with the inverter channels the exchanging recurrence sounds and produces an excellent sinusoidal AC waveform appropriate for the committed burdens.

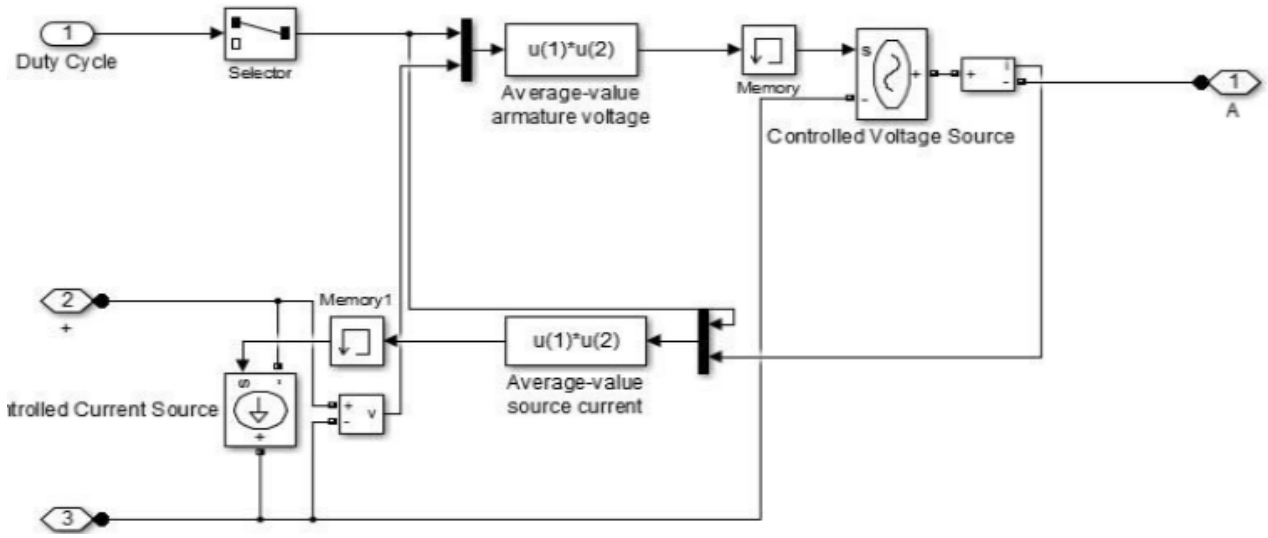

Figure 5: Internal SIMULINK Diagram of Chopper

C. PID Controller

This is the control loop feedback technique that used in industrial control system and a variety of other application requiring continuously modulated control. In the PID controller there are three term proportional- integral-derivative.

In this paper PID controller control the temperature of the fuel cell stack system. This temperature sensor in controlled by using thermocouple or RTD as input and compare with the actual temperature to the desired control temperature or a set point or it will provided an output to control element. In this paper the control set pint temperature is 338oC. A dc bus capacitive energy set pint was defined by YbusREF. This is control a flow rate H2 and air (O2). This is shown in figure 4.

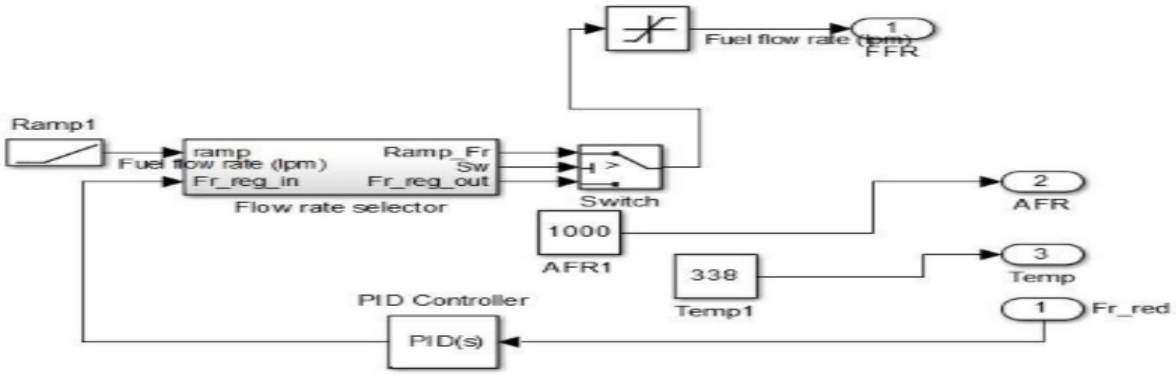

Figure 6: PID Controller

IV. SMART ENERGY

As per the "International Electrotechnical Commission" (IEC), "Savvy Grid is the idea of modernizing the electric lattice. The Smart Grid is coordinating the electrical and data advances in the middle of any purpose of Generation and any purpose of Consumption".

According to "NIST" has moreover developed the Smart Grid Conceptual Model which gives an anomalous state framework to the sharp cross section that portrays seven key zones: Bulk Generation, Transmission, Distribution, Customers, Operations, Markets and Service Providers where control quality has been acknowledged as a crucial part in the Smart Grid Network. The amount of system structures like Wind Energy Systems and Photovoltaic are by and by sharp more into the grid and furthermore the amounts of non-coordinate burdens are moreover growing. Keen vitality matrices potential assume an extraordinary part for the biogas. Biogas framework might be help to build the extents of variable on inexhaustible power on the power network by utilizing of two unique advances [10].

- Biogas structures which augment the era of energy at the period of ubiquity for the power, or store the biogas unexpectedly at the period of low power ask.
- This take steps to biogas plant if the less enthusiasm for control low than supply of energy to system, pleasing surplus energy to gas.

Numerous segments in a telecom control arrangement can be either associated into the brilliant matrix world or can be a direct part of the brilliant matrix. The present power frameworks, counting energy components, have insightful controllers and system interfaces bringing about keen, remotely reasonable gadgets with interfaces that give standard conventions to Machine to Machine Interfaces or Human to Machine Interfaces [9].

A Smart Energy arrangement in telecom must have the capacity to be overseen by means of conventional operations strategies. In the models displayed in this paper, the operations focus ought to have the capacity to control and deal with various power frameworks at any given time utilizing direct charges or preset contents [8]. When utilizing little control frameworks like energy units at cell locales there is should be ready to oversee possibly many gadgets to move up to a control level that has any kind of effect on the matrix. Five or ten locales at 6kW won't intrigue the utility and truly does nothing for the broadcast communications administrator's vitality utilization.

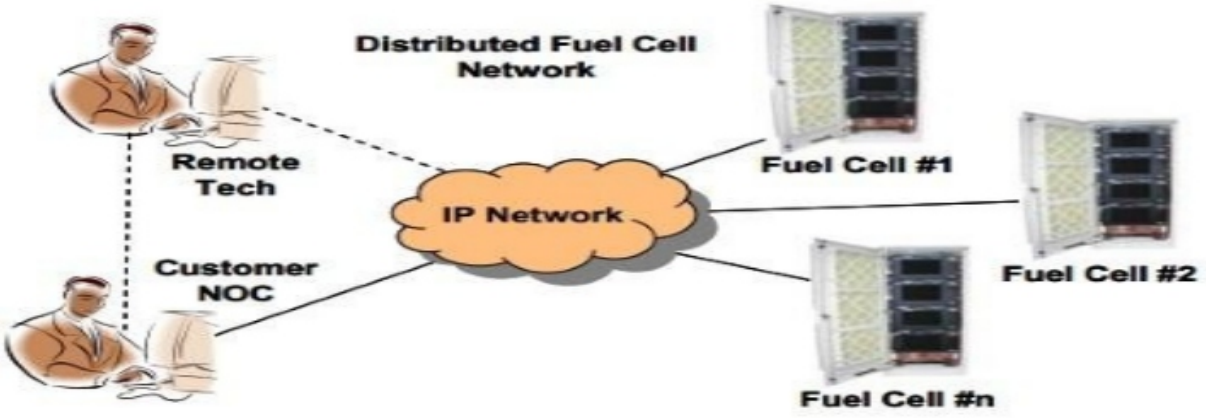

Figure 7: Network of fuel Cell [8]

Organized and gathering of energy components that are overseen from the Network Operations Center (NOC) or by an outsider administrations organization. At the point when there is a need to create control, the summon can be issued by means of the system to begin era, stop era and assemble measurements about the generation of vitality [8]. Fuel cell IP network are connected to the different generation of the fuel cell in the term of distributed fuel network and connect remote tech and customer NOC as shown in figure 7.

V. SIMULATION RESULT

A. DC Bus Voltage:

The main task to convert the regulate voltage to the constant DC voltage from 48V to 100V. This is boost done by using the DC/DC converter. The stability of voltage checked. Figure 8 is shown that the boost voltage.

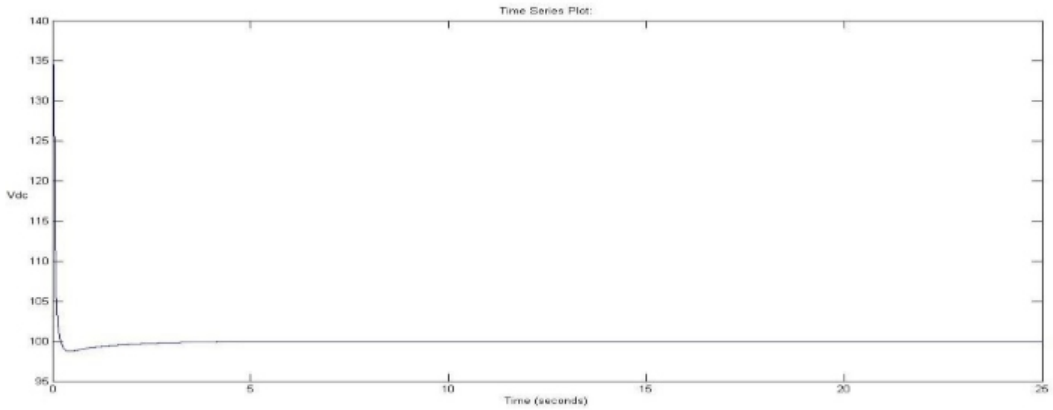

Figure 8: DC/DC Converter Bus DC Voltage

B. Power Flow:

The output power can be controlled by the converter, and under the reference control requests, the yield energy of fuel cell takes after the power requests. The model of energy unit control plant utilized as a part of the paper is the power device of PEM what's more, gas turbine. It implies that energy component control plant creates more energy to give the matrix at beginning time, and the gas turbine produces control gradually due to the dormancy of gas turbine. In spite of the fact that there are some distinction between the reference and reenactment, the model tracks the reference nearly. The DC power flow of the from the system is reach up to the 6kW as show in figure 9.

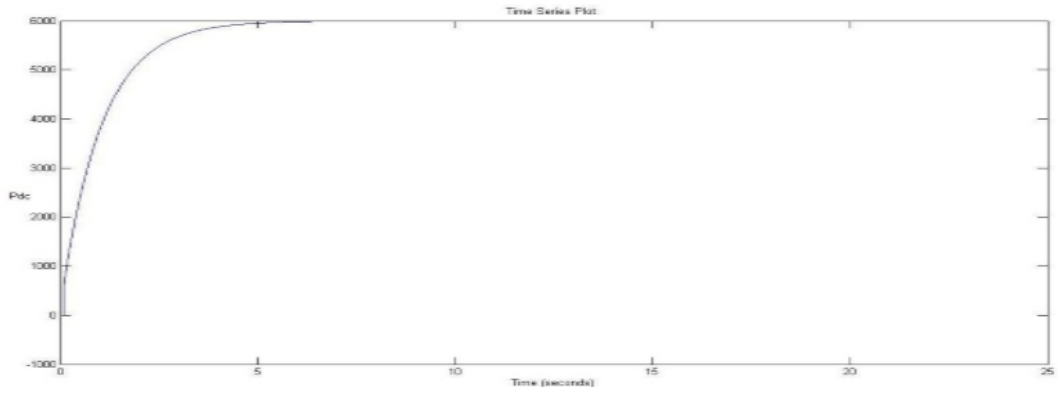

Figure 9: DC Power Flow

C. Efficiency and Utilization:

The electrical effectiveness of cogeneration frameworks is an essential paradigm in biogas ventures [12]. This kind of extend is financially practical just if there is a huge need of warmth close to the power plant. The diverse current sorts of power module cogeneration framework create arrived at the midpoint of half of their aggregate control into warm and their electrical proficiency is up to 60% [11].

The maximum efficiency limit of a fuel cell, often referred to as the thermodynamic efficiency, is calculated as follows.

$$\text{Maximum Efficiency} = \eta_{\max} = \frac{\Delta G^{\circ}_{rxn,T}}{\Delta H^{\circ}_{rxn,298}} \times 100$$

But in this paper the efficiency of this model near to the 55.56% that near about the maximum. As shown in figure 10. The industrialization of cogeneration with high electrical productivity, the PEM framework, could in this manner serve numerous new power module ventures.

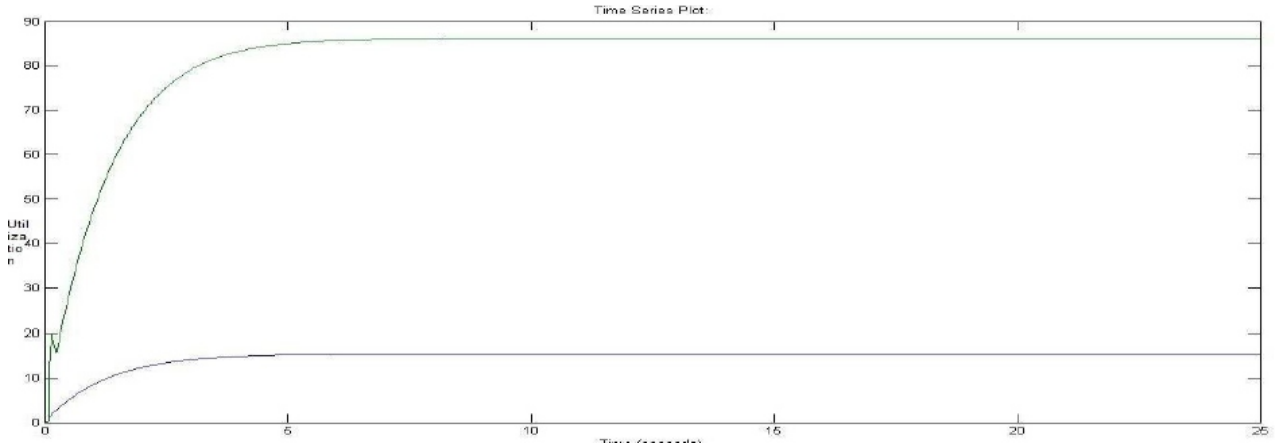

Figure 10: Efficiency of the fuel Cell Stack at the level of 6kW

CONCULUSION

In this paper Smart energy programs come in numerous varieties and are developing in prominence because of progressing electrical network issues. Overall electrical request keeps on expanding bringing about limit deficiencies and strain on network foundation. Disappointments also, flimsiness is inescapable without rectifications. Smart energy also, request side projects are venture toward amendment. Smart energy arrangements alongside savvy gadgets offer important apparatuses for the media communications administrator to use their reinforcement control resources for monetary and natural esteem. The administrators can turn into a "prosumer" both creating and expending energy. They are presently dynamic in the arrangement rather than absolutely a buyer of assets. The present power devices offer a feasible answer for help the need of reinforcement control and the smart energy arrangements. The broadcast communications administrator has a decision: they can purchase a vigorous reinforcement control arrangement and get a smart energy arrangement or they can purchase a smart energy arrangement and get a reinforcement control arrangement as a side advantage.

In this paper improve the efficiency of the fuel power model. Also improve in the utilization of voltage and power. This system is used in the distribution system to connect to the grid at rural area or hilly area.

REFERENCE

[1] HYDROGEN ENERGY AND FUEL CELLS IN INDIA – A WAY FORWARD Report prepared by Steering Committee on Hydrogen Energy and Fuel Cells, Ministry of New and Renewable Energy, Government of India, New Delhi June, 2016

[2] Kavya V R, Padmavathy K S, Shaneeth M "Steady State Analysis and Control of PEM Fuel Cell Power Plant", 2013 International Conference on Control Communication and Computing (ICCC) 978-1-4799-0575-1/13/2013 IEEE

[3] J. Larminie and A. Dicks: "Fuel Cell Systems Explained". 2nd ed, J.Wiley & Sons, England, 2003.

[4] R. F. Mann, J. C. Amphlett, M. A. I. Hooper, and et al. "Development and application of a generalized steady-state electrochemical model for a PEM fuel cell". Journal of Power Sources, 2000, vol. 86.

[5] J. M. Corr ̂ea, F. A. Farret, and L. N. Canha, "An Analysis of the Dynamic Performance of Proton Exchange Membrane Fuel Cells Using an Electrochemical Model". In: IECON, 2001.

[6] Samrat Deb Chouudhury, Vinay Mohan Bhardwaj, Nandikesan P,Surajeet Mohanty,Shaneeth M,Kamalakaran K P,'Control "Strategy for PEM Fuel cell power plant",Lithium Ion and Fuel cell Division, Vikram Sarabhai Space Centre

[7] Chief Operating Officer ReliOn Spokane, Joe Blanchard, "Smart Energy Solutions Using Fuel Cells"

[8] J.L. Rodrigues Amendo, "Spain's Example of Solving Grid Stabilization Issues," www.renewableenergyworld.com, October 2010.

[9] University of Southern Denmark Esbjerg, NielsBohrsVej 9-10, DK-6700 Esbjerg, Denmark, Teodorita Al Seadi, DominikRutz, Heinz Prassl, Michael Köttner, Tobias Finsterwalder, Silke Volk, Rainer Janssen, ISBN 978-87- 992962-0-: Copyright © 2008"

[10] Tobias Persson, Jerry MurPhy, Anna-Karin JAnnAsch, eoin Ahern, Jan LiebeTrAu, Marcus TroMMLer, Jeferson ToyAMA "A perspective on the potential role of biogas in smart energy grids"

[11] C. Walla and W. Schneeberger, "The optimal size for biogas plants," Biomass and Bioenergy, vol. 32, no. 6, pp. 551–557, Jun. 2008.

[12] Sylvain BAUDOIN Ionel VECHIU,Haritza CAMBLONG, Jean-Michel VINASSA," "Analysis and validation of a biogas hybrid SOFC/GT emulator" 978-1-4799-5857-3/14/2014 IEEE

[13] J. Larminie, A. Dicks, and M. McDonald, "Fuel cell systems explained," 2003.

Instructions for Authors

Essentials for Publishing in this Journal

1 Submitted articles should not have been previously published or be currently under consideration for publication elsewhere.

2 Conference papers may only be submitted if the paper has been completely re-written (taken to mean more than 50%) and the author has cleared any necessary permission with the copyright owner if it has been previously copyrighted.

3 All our articles are refereed through a double-blind process.

4 All authors must declare they have read and agreed to the content of the submitted article and must sign a declaration correspond to the originality of the article.

Submission Process

All articles for this journal must be submitted using our online submissions system. http://enrichedpub.com/ . Please use the Submit Your Article link in the Author Service area.

Manuscript Guidelines

The instructions to authors about the article preparation for publication in the Manuscripts are submitted online, through the e-Ur (Electronic editing) system, developed by **Enriched Publications Pvt. Ltd**. The article should contain the abstract with keywords, introduction, body, conclusion, references and the summary in English language (without heading and subheading enumeration). The article length should not exceed 16 pages of A4 paper format.

Title

The title should be informative. It is in both Journal's and author's best interest to use terms suitable. For indexing and word search. If there are no such terms in the title, the author is strongly advised to add a subtitle. The title should be given in English as well. The titles precede the abstract and the summary in an appropriate language.

Letterhead Title

The letterhead title is given at a top of each page for easier identification of article copies in an Electronic form in particular. It contains the author's surname and first name initial .article title, journal title and collation (year, volume, and issue, first and last page). The journal and article titles can be given in a shortened form.

Author's Name

Full name(s) of author(s) should be used. It is advisable to give the middle initial. Names are given in their original form.

Contact Details

The postal address or the e-mail address of the author (usually of the first one if there are more Authors) is given in the footnote at the bottom of the first page.

Type of Articles

Classification of articles is a duty of the editorial staff and is of special importance. Referees and the members of the editorial staff, or section editors, can propose a category, but the editor-in-chief has the sole responsibility for their classification. Journal articles are classified as follows:

Scientific articles:

1. Original scientific paper (giving the previously unpublished results of the author's own research based on management methods).

2. Survey paper (giving an original, detailed and critical view of a research problem or an area to which the author has made a contribution visible through his self-citation);

3. Short or preliminary communication (original management paper of full format but of a smaller extent or of a preliminary character);

4. Scientific critique or forum (discussion on a particular scientific topic, based exclusively on management argumentation) and commentaries. Exceptionally, in particular areas, a scientific paper in the Journal can be in a form of a monograph or a critical edition of scientific data (historical, archival, lexicographic, bibliographic, data survey, etc.) which were unknown or hardly accessible for scientific research.

Professional articles:

1. Professional paper (contribution offering experience useful for improvement of professional practice but not necessarily based on scientific methods);
2. Informative contribution (editorial, commentary, etc.);
3. Review (of a book, software, case study, scientific event, etc.)

Language

The article should be in English. The grammar and style of the article should be of good quality. The systematized text should be without abbreviations (except standard ones). All measurements must be in SI units. The sequence of formulae is denoted in Arabic numerals in parentheses on the right-hand side.

Abstract and Summary

An abstract is a concise informative presentation of the article content for fast and accurate Evaluation of its relevance. It is both in the Editorial Office's and the author's best interest for an abstract to contain terms often used for indexing and article search. The abstract describes the purpose of the study and the methods, outlines the findings and state the conclusions. A 100- to 250- Word abstract should be placed between the title and the keywords with the body text to follow. Besides an abstract are advised to have a summary in English, at the end of the article, after the Reference list. The summary should be structured and long up to 1/10 of the article length (it is more extensive than the abstract).

Keywords

Keywords are terms or phrases showing adequately the article content for indexing and search purposes. They should be allocated heaving in mind widely accepted international sources (index, dictionary or thesaurus), such as the Web of Science keyword list for science in general. The higher their usage frequency is the better. Up to 10 keywords immediately follow the abstract and the summary, in respective languages.

Acknowledgements

The name and the number of the project or programmed within which the article was realized is given in a separate note at the bottom of the first page together with the name of the institution which financially supported the project or programmed.

Tables and Illustrations

All the captions should be in the original language as well as in English, together with the texts in illustrations if possible. Tables are typed in the same style as the text and are denoted by numerals at the top. Photographs and drawings, placed appropriately in the text, should be clear, precise and suitable for reproduction. Drawings should be created in Word or Corel.

Citation in the Text

Citation in the text must be uniform. When citing references in the text, use the reference number set in square brackets from the Reference list at the end of the article.

Footnotes

Footnotes are given at the bottom of the page with the text they refer to. They can contain less relevant details, additional explanations or used sources (e.g. scientific material, manuals). They cannot replace the cited literature.

The article should be accompanied with a cover letter with the information about the author(s): surname, middle initial, first name, and citizen personal number, rank, title, e-mail address, and affiliation address, home address including municipality, phone number in the office and at home (or a mobile phone number). The cover letter should state the type of the article and tell which illustrations are original and which are not.

Address of the Editorial Office:

Enriched Publications Pvt. Ltd.
S-9,IInd FLOOR, MLU POCKET,
MANISH ABHINAV PLAZA-II, ABOVE FEDERAL BANK,
PLOT NO-5, SECTOR -5, DWARKA, NEW DELHI, INDIA-110075,
PHONE: - + (91)-(11)-45525005